PALEOCEANOGRAPHY, VOL. 9, NO. 6, PAGES 781-798, DECEMBER 1994

Photosynthetic fractionation of ^{13}C and concentrations of dissolved CO_2 in the central equatorial Pacific during the last 255,000 years

John P. Jasper[1] and J. M. Hayes
Biogeochemical Laboratories, Indiana University, Bloomington

A. C. Mix and F. G. Prahl
College of Oceanography, Oregon State University, Corvallis

Abstract. Carbon isotopically based estimates of CO_2 levels have been generated from a record of the photosynthetic fractionation of ^{13}C ($\equiv \varepsilon_p$) in a central equatorial Pacific sediment core that spans the last ~255 ka. Contents of ^{13}C in phytoplanktonic biomass were determined by analysis of C_{37} alkadienones. These compounds are exclusive products of Prymnesiophyte algae which at present grow most abundantly at depths of 70-90 m in the central equatorial Pacific. A record of the isotopic compostion of dissolved CO_2 was constructed from isotopic analyses of the planktonic foraminifera *Neogloboquadrina dutertrei,* which calcifies at 70-90 m in the same region. Values of ε_p, derived by comparison of the organic and inorganic δ values, were transformed to yield concentrations of dissolved CO_2 ($\equiv c_e$) based on a new, site-specific calibration of the relationship between ε_p and c_e. The calibration was based on reassessment of existing ε_p versus c_e data, which support a physiologically based model in which ε_p is inversely related to c_e. Values of PCO_2, the partial pressure of CO_2 that would be in equilibrium with the estimated concentrations of dissolved CO_2, were calculated using Henry's law and the temperature determined from the alkenone-unsaturation index $U^{K'}_{37}$. Uncertainties in these values arise mainly from uncertainties about the appropriateness (particularly over time) of the site-specific relationship between ε_p and $1/c_e$. These are discussed in detail and it is concluded that the observed record of ε_p most probably reflects significant variations in ΔpCO_2, the ocean-atmosphere disequilibrium, which appears to have ranged from ~110 µatm during glacial intervals (ocean > atmosphere) to ~60 µatm during interglacials. Fluxes of CO_2 to the atmosphere would thus have been significantly larger during glacial intervals. If this were characteristic of large areas of the equatorial Pacific, then greater glacial sinks for the equatorially evaded CO_2 must have existed elsewhere. Statistical analysis of air-sea pCO_2 differences and other parameters revealed significant ($p < 0.01$) inverse correlations of ΔpCO_2 with sea surface temperature and with the mass accumulation rate of opal. The former suggests response to the strength of upwelling, the latter may indicate either drawdown of CO_2 by siliceous phytoplankton or variation of $[CO_2]/[Si(OH)_4]$ ratios in upwelling waters.

Introduction

Atmospheric CO_2 levels depend on the balance of CO_2 flowing into and out of the world ocean and terrestrial ecosystems. To a first approximation, equatorial regions of the contemporary oceans are supersaturated with CO_2 relative to the atmosphere, subpolar regions approach air-sea equilibrium, and polar regions are undersaturated [*Volk and Bacastow*, 1989; *Tans et al.*, 1990; *Murphy et al.*, 1991]. The supersaturation of CO_2 in equatorial waters results in a large efflux of CO_2 to the atmosphere, and this is largely balanced by an influx of CO_2 into subpolar-to-polar waters. Because of its high productivity, non zero surface nutrients, present disequilibrium with the atmosphere, and large changes in paleotemperatures, the equatorial Pacific upwelling zone has long been suspected of participating in the atmospheric CO_2 changes associated with glacial-interglacial cycles.

To define better mechanisms by which oceanic and atmospheric levels of CO_2 change, we must delineate paleoceanic sources and sinks of carbon dioxide. A mechanism for the maintenance of oceanic PCO_2 and atmospheric pCO_2, based the on the regulation of CO_2 levels by the growth and erosion of coral reefs, has recently been positively reassessed in light of new reef-carbonate and ice core CO_2 data [*Berger*, 1982; *Opdyke and Walker*, 1992]. A paleoceanographic CO_2 proxy based on the $\delta^{13}C$ difference

[1]Now at Department of Marine Sciences, University of Connecticut, Groton.

Paper number 94PA02116.
0883-8305/94/94PA-02116$10.00

between planktonic and benthic foraminiferal carbonates ($\Delta\delta^{13}C_{p\text{-}B}$) was interpreted to record the intensity of biological productivity via the preferential drawdown of $^{12}CO_2$ relative to $^{13}CO_2$ [*Broecker*, 1982; *Shackleton et al.*, 1983; *Shackleton and Pisias*, 1985]. Because the $\Delta\delta^{13}C_{p\text{-}B}$ proxy reconstructs the ^{13}C gradient within the water column, it gives important insights into the internal circulation of ocean. More recently, a class of paleo-PCO_2 indicators has been developed to estimate concentrations of dissolved CO_2 ($\equiv c_e$, where the subscript e specifies the concentration external to a photosynthetic cell) in preexisting surface waters. On the basis of the carbon isotopic fractionation caused by photosynthetic fixation of CO_2 ($\equiv \varepsilon_p$), these PCO_2 proxies have been developed using bulk organic carbon from sediments [*Arthur et al.*, 1985] and the contemporary water column [*Rau et al.*, 1991, 1992; *Francois et al.*, 1993] and individual biomarker compounds (geoporphyrins: *Popp et al.* [1989]; long-chain alkenones: *Jasper and Hayes* [1990]; phytosterols: *Wakeham et al.* [1993]; for a review of factors affecting levels of ^{13}C in sedimentary compounds: see *Hayes* 1993). Efforts are being made to understand better the relationship between c_e and the $\delta^{13}C$ of phytoplanktonic carbon [*e.g., McCabe*, 1985; *Rau et al.*, 1991, 1992; *Freeman and Hayes*, 1992; *Hayes and Jasper*, 1993; *Francois et al.*, 1993; *Goericke et al.*, 1993].

Ice cores record the composition of paleoatmospheric gases in ice-entrapped vesicles, whereas the ε_p method derives its signal from the $\delta^{13}C$ of biogenic components from the oceanic water column as recovered from deep-sea sediment cores. Each of these techniques has a characteristic spatial scale of relevance. Ice cores provide global records because of rapid atmospheric circulation mixing. Provided that factors regulating carbon demand (discussed below) are relatively constant, the ε_p method provides a record of c_e at a particular site and at the depth at which the C-fixing organisms grew. Applying the ε_p method in oceanic regions that approach air-sea equilibrium for CO_2 allows estimation of paleoatmospheric pCO_2, but only if the producers of whatever biomarkers were employed recorded conditions at the sea surface. Accordingly, more must be learned about the depth habitats of the organisms that produce estimators of ε_p. In areas of air-sea disequilibrium, sources and sinks for CO_2 can be delineated provided that atmospheric pCO_2 is known. To a first approximation, the disequilibrium can then be accounted for in terms of the balance of paleocirculation (c_e and nutrient upwelling), paleoproductivity (drawdown of c_e), and the kinetics of air-sea exchange of CO_2.

In the present study a record of ε_p has been based on isotopic differences between an $n\text{-}C_{37}$ alkadienone synthesized by prymnesiophyte algae and carbonate tests of planktonic foraminifera (*N. dutertrei*). Isotopic analysis of the alkenone allows estimation of the $\delta^{13}C$ of prymnesiophyte biomass, while that of the foraminiferan monitors, with allowance for equilibrium fractionations and vital effects, the $\delta^{13}C$ of dissolved CO_2. Our purpose has been to develop a record of CO_2 levels in a central equatorial Pacific upwelling region. From the outset we follow *Skirrow* [1975] in using PCO_2 to denote equilibrium partial pressures calculated from concentrations of dissolved CO_2 via Henry's law and pCO_2 to denote the partial pressure of CO_2 in a given atmosphere, a parameter presumably monitored directly by ice core records [e.g., *Barnola et al.*, 1987; *Jouzel et al.*, 1993]. This site was chosen to monitor variations in paleoceanic PCO_2 in the equatorial Pacific cold tongue, currently a zone of upwelling with high equilibrium PCO_2 relative to the overlying atmosphere [*Volk and Bacastow*, 1989; *Tans et al.*, 1990]. We seek to test the hypothesis that glacial to interglacial changes in oceanic circulation or productivity in this upwelling zone contributed to late Quaternary variations in paleoceanic PCO_2 and, perhaps, paleoatmospheric pCO_2.

Samples and Methods

Site

A 330-cm gravity core (W8402A-14GC) was raised from the abyssal plain of the central equatorial Pacific at MANOP site C (0°57.2'N, 138°57.3'W; 4287 m) in 1984 from the *R/V Wecoma* (Figure 1). The core was split lengthwise, and both halves were stored at 4°C at the Oregon State University core repository until subsampled in 1987-1989 for organic geochemical research. All MANOP site C data in this study derive from this sediment core.

The sediments are composed primarily of calcite with minor amounts of opal and minimal continental debris, characteristic of sediments throughout the abyssal plain of the central equatorial Pacific [*Lyle et al.*, 1988]. An initial age scale for this core was assigned by oxygen isotope stratigraphy using *Globoratalia tumida* [*Murray*, 1987] and is refined here using a *Cibicidoides wuellerstorfii* oxygen isotope record via the SPECMAP time frame [*Imbrie et al.*, 1989], discussed below.

The $\delta^{18}O$ and $\delta^{13}C$ of C. wuellerstorfii and N. dutertrei

The benthic foraminiferan *C. wuellerstorfii* was analyzed for stratigraphic purposes. The planktonic foraminifera *N. dutertrei* was chosen to monitor the $\delta^{13}C$ of dissolved inorganic carbon because in the equatorial Pacific it calcifies near the chlorophyll maximum [*Ravelo et al.*, 1990], at approximately the same depths that prymnesiophytes grow. This planktonic species has no algal symbionts that influence $\delta^{13}C$ composition [*Hemleben et al.*, 1989] and is very abundant in this area. At 140°W in the equatorial Pacific, concentrations of the $C_{37:2}$ alkenones show concentration maxima at ~70-90 m at ~2°-6° N and S of the equator [*Fluegge*, 1994], coincident with the depth of the maximum vertical density contrast in the pycnocline [*Levitus*, 1982].

Foraminiferal carbonates were analyzed at Oregon State University using a Finnigan-MAT 251 dual-inlet mass spectrometer equipped with an AutoprepSystems carbonate device. In this system, CO_2 is prepared by reaction of carbonates with ~100% phosphoric acid at 90°C. During 1991 the standard deviations of $\delta^{18}O$ and $\delta^{13}C$ analyses on laboratory standard calcite were ± 0.06 and ± 0.04 ‰, respectively, (n = 286); calibration to the Pee Dee Belemnite (PDB) scale was made through the National Institute of Standards and Technology NBS-20 carbonate standard with precision of ± 0.03‰ for $\delta^{18}O$ and ± 0.03‰ for $\delta^{13}C$.

Ages are based on visual correlation of the benthic foraminiferal oxygen isotope record with the SPECMAP

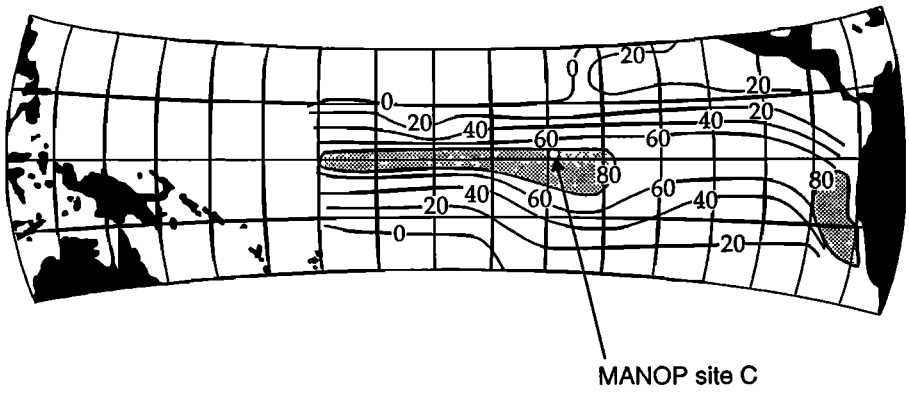

Figure 1. Map of equatorial Pacific showing the location of MANOP site C (0°57.2'N, 138°57.3'W; 4287 m) and the distribution of excess CO_2 partial pressures (μatm) in surface waters. Although a more recent map of the air-sea difference in CO_2 in this region [*Murray et al.*, 1993] shows somewhat lower ΔpCO_2 values at 140°W on the equator, the orientation of MANOP site C relative to the coasts and zonal patterns of ΔpCO_2 change in the map are useful here (modified from *Broecker and Peng* [1982]).

"stacked" benthic foraminiferal $\delta^{18}O$ timescale [*Martinson et al.*, 1987]. Comparisons to the Vostok ice core CO_2 record are based on correlation of lithogenic dust fluxes in the ice cores and nonbiogenic sediments in southern ocean marine cores [*Petit et al.*, 1990].

Alkenones

Samples. The core was sampled at ~5-cm intervals in 1984. Given a sedimentation rate of 1.3 to 1.4 cm/kyr based on our correlation to the SPECMAP $\delta^{18}O$ timescale [*Imbrie et al.*, 1984], this implies a time interval of ~4 kyr. Profiles of ^{14}C activity measured in bulk carbonate material from another core collected at site C indicate bioturbation depths of ~7 cm [*Emerson et al.*, 1987]. Any individual sample may represent an average of 4-5 kyr of accumulation, which is approximately equal to the error in the calibration of the timescale [*Imbrie et al.*, 1984]. With these samples from a core from an area with a relatively low sedimentation rate, we cannot address the possibility of high-frequency variations in CO_2 that have been detected in ice cores [*Stauffer et al.*, 1984].

Analyses. Fractions for gas chromatographic analysis were isolated at Oregon State University using previously described liquid chromatographic methods [*Prahl et al.*, 1989]. The precision of measurement of $U^{K'}_{37}$ corresponds to an accuracy of ± 0.5°C in temperature [*Prahl et al.*, 1989]. Selected fractions were analyzed by electron-impact (70 eV) gas chromatography-mass spectrometry to confirm the presence of the alkenones and the absence of interfering compounds.

The carbon isotopic composition of heptatriconta-15,22-dien-2-one, the major C_{37} alkadienone [*de Leeuw et al.*, 1980] henceforth noted as $C_{37:2}$, was determined by isotope-ratio-monitoring gas chromatography-mass spectrometry (irmGCMS) [*Hayes et al.*, 1990; *Freeman et al.*, 1990]. Coinjected *n*-alkanes (C_{38} and C_{41}) were employed as isotopic standards. The precision and accuracy obtained in each run were internally checked by analysis of two other coinjected *n*-alkanes (C_{36} and C_{37}). Performance of the instrument was monitored by comparison of δ values obtained by combustion of the internal standard *n*-alkanes and by injection of CO_2 gas calibrated against NBS standards. A typical ion-current recording is shown in Figure 2. The standard deviation of $\delta_{37:2}$ values, determined by pooling of replicate alkenone measurements, is typically ± 0.30‰.

Prior to carbon isotopic analysis, each alkenone fraction was screened to determine whether significant quantities of methylhexatriaconta-14,21-dienoate [*Prahl et al.*, 1988] were present. This compound, henceforth noted as C_{36me}, co-elutes with $C_{37:2}$ and, if not removed, can lead to inaccurate analyses. Accordingly, if preliminary gas chromatographic analyses revealed concentrations of C_{36me} exceeding 3% of that of $C_{37:2}$, the alkenone-containing fraction was saponified to allow removal of the interfering ester.

Saponification and purification of alkenone fractions. Extracts containing unresolved alkenoates were transferred in hexane to a 1.0-mL conical reaction vial, and the hexane was evaporated using a stream of N_2 gas. A 0.3-mL aliquot of 0.5 N KOH in CH_3OH/H_2O (95/5, v/v) was added, the vial was tightly capped, and the solution was vortex-mixed for 30 seconds prior to heating at 95°C for 2 hours. The mixture was cooled to room temperature and extracted with hexane (3 × 0.5 mL). The extracts were combined and the solvent evaporated. A purified alkenone fraction was recovered by eluting the extract with solvents of increasing polarity (*n*-hexane to methylene chloride) through a column of silica gel (1 g, 5% deactivated 100-200 mesh, Mallinckrodt Company) topped with ~0.5 g of anhydrous Na_2SO_4.

Calculations

The measurable isotopic difference, that between alkenones and foraminiferal calcite, incorporates contributions associated with (1) the exchange of C between carbonate minerals and dissolved CO_2, (2) the assimilation and photosynthetic reduction of CO_2 (i.e., "fixation") to provide the first intracellular organic product, and (3) the biosynthesis of alkenones. Only for the second of these processes is isotopic fractionation thought to depend on c_e, and the definition of ε_p (equation (4), below) associates it specifically

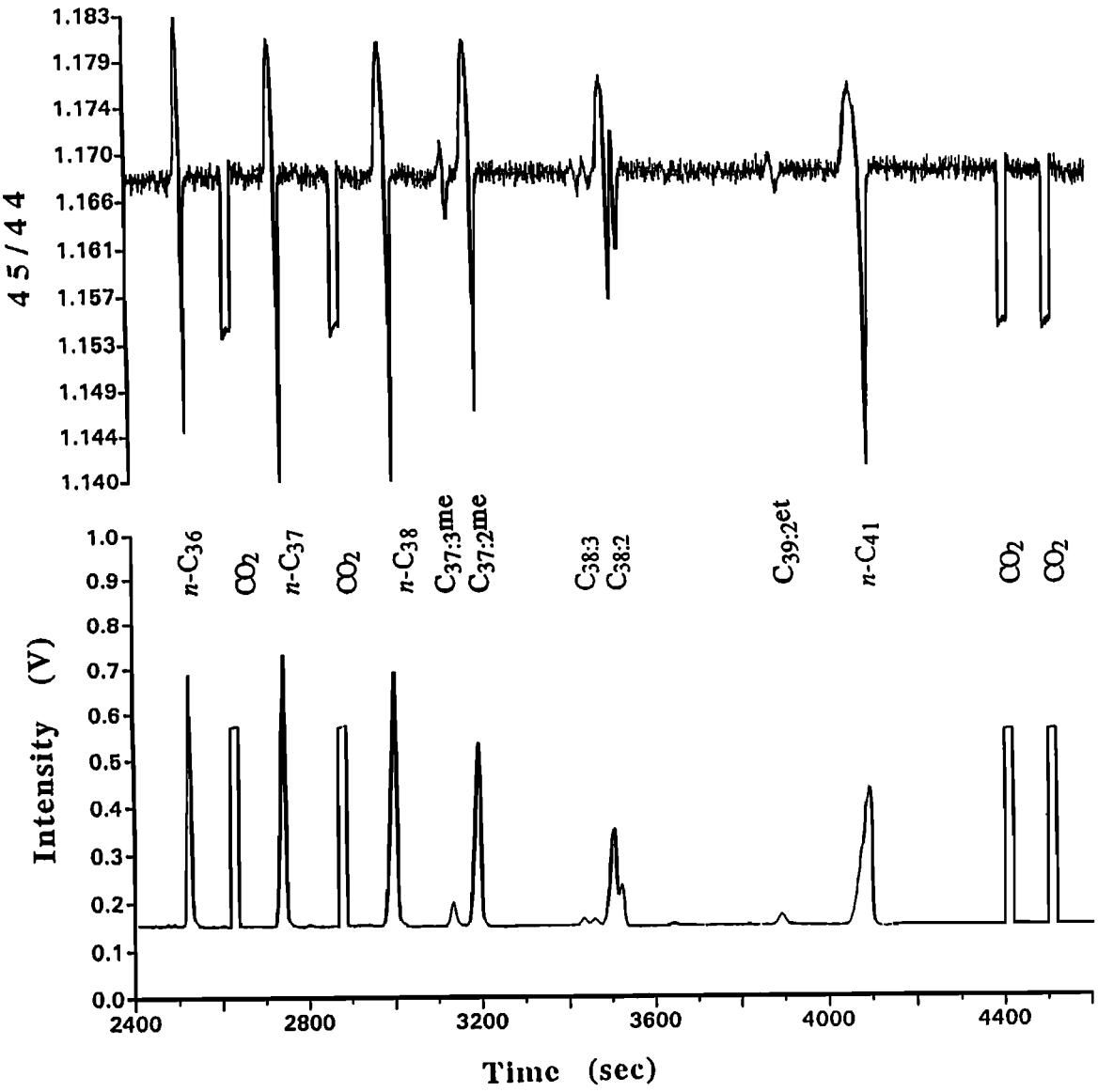

Figure 2. Chromatograms of the mass-45/mass-44 ratio (above) and total mass-44 ion current generated from the ketone fraction of a MANOP Site C extract (50.5 cm, 25.5 kyrBP). The long-chain alkenones are identified as follows: $C_{37:3}$me indicates heptatricontatrien-2-one, $C_{37:2}$me indicates heptadicontadien-2-one ($\delta^{13}C_{37:2}$ = -25.4 ± 0.4‰), $C_{38:3}$ indicates sequentially octatriacontatrien-3-one and octatriacontatrien-2-one, $C_{38:2}$ indicates sequentially octatriacontadien-3-one and octatriacontadien-2-one, and $C_{39:2}$et indicates nonatriacontadien-3-one. Internal standard *n*-alkanes (*n*-C_{36}, *n*-C_{37}, *n*-C_{38}, *n*-C_{41}), and external CO_2 standards (square peaks) permitted isotopic standardization of δ-alkenone measurements (see samples and methods section in text). Only the $\delta^{13}C$ values of the $C_{37:2}$ alkenone are reported in this study because the other alkenones typically yielded < 0.1 V intensity or coeluted with adjacent compounds.

with this process. Fortunately, the isotopic differences associated with the first and third processes can be estimated from separate lines of evidence, and values of ε_p thus determined. Two assumptions are involved: (1) that isotopic equilibrium prevails within the dissolved CO_2-carbonate system, even within the boundary layer of a photosynthesizing cell, and (2) that biosynthetic isotope effects observed in laboratory cultures accurately reflect those occurring in the natural environment. Either or both of these assumptions may be imperfect, but any approach to dissection of these processes is better than none at all. The alternative would be to attempt calibration and use of a c_e-fractionation relationship based on the alkenone-calcite difference, and this would be unrealistic and misleading. Not only is the fractionation associated with processes other than fixation not dependent on c_e but that between calcite and dissolved CO_2, whether it occurs at equilibrium or not, is strongly temperature-dependent. Use of the gross isotopic difference

would therefore combine and confound temperature- and CO_2-related variations. Because the raw data, the isotopic compositions of the foraminiferal calcites and the alkenones, are tabulated here, any subsequent information allowing improved treatment of these assumptions can be readily taken into account.

Further points are best considered after introduction of the quantitative framework, which is outlined in Figure 3 and discussed below. The following definitions are pertinent.

$\varepsilon_{m/d}(T)$: the temperature-dependent fractionation factor relating ^{13}C contents of mineral calcite (m) and dissolved CO_2 (d) at equilibrium.

$$\varepsilon_{m/d} \equiv (\alpha_{m/d} - 1)10^3 = [(\delta_m + 1000)/(\delta_d + 1000) - 1]10^3 \quad (1)$$

where δ_m and δ_d are the carbon isotopic compositions of calcite carbon and of carbon in CO_2(aq), respectively.

$\Delta_{m/f}$: the isotopic difference between equilibrated calcite and foraminiferal calcite (i.e., a "vital effect," which would be zero if equilibrium prevailed in the biological system).

$$\Delta_{m/f} = \delta_m - \delta_f \quad (2)$$

where δ_f is the measured carbon isotopic composition of foraminiferal calcite. We assume that $\Delta_{m/f}$ is constant through time, although this may not be strictly true [*Spero et al.*, 1991].

δ_P: the estimated carbon isotopic composition of Prymnesiophyte biomass, which, due to intracellular isotope effects accompanying biosynthesis, is distinct from the measured isotopic composition of $C_{37:2}$. This definition of δ_P removes non-c_e-dependent, biosynthetic fractionations from the signal that is interpreted in terms of variations in c_e.

$$\delta_P = \delta_{37:2} + \Delta_{P/l} \quad (3)$$

where $\delta_{37:2}$ is the carbon isotopic composition of $C_{37:2}$ and $\Delta_{P/l}$ is the isotopic difference between total biomass and $C_{37:2}$ (the *P* and *l* refer to primary product and lipid, respectively). Because $\Delta_{P/l}$ is added to $\delta_{37:2}$ during both calibration and application of the ε_P-PCO_2 relationship, any errors in the value assigned to it will cancel. This term is still worth defining and considering separately for two reasons. First, the alternative is to hide the intracellular fractionation by combining it with the fractionation associated with fixation of carbon. This is unrealistic and would lead to incorrect views of the relative magnitude of changes in ε_P. Second, this approach has the effect of establishing δ_P as a reference point, facilitating comparison of these results to others based on POC. The approach can be readily extended to investigations based on other photosynthetic biomarkers and would provide a common basis for intercomparisons. Here we adopt $\Delta_{P/l} = 3.8‰$ [*Jasper and Hayes*, 1990]. Although this value

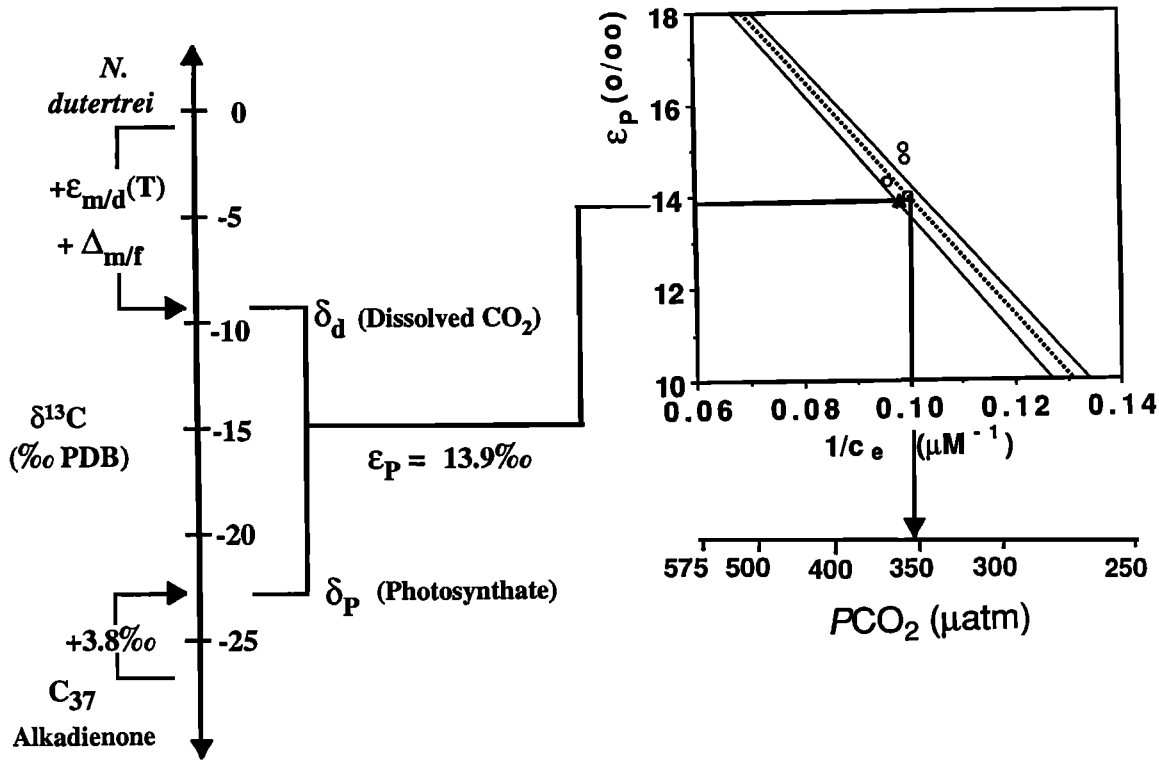

Figure 3. Diagram outlining the calculation of equilibrium, or paleoceanic, PCO_2 values from the photosynthetic fractionation of CO_2 (ε_P). From the carbon isotopic compositions of a planktonic foraminiferan (namely, *N. dutertrei*) and Prymnesiophyte microalgae (via a C_{37} alkadienone), values of ε_P are reconstucted. Calibration of ε_P points against $1/c_e$ allows reconstruction of equilibrium PCO_2 values from sedimentary components. The calibration used here ($\varepsilon_P = 27 - 130/c_e$, the middle dotted line) was generated by consideration of fractionations displayed by equatorial Pacific water column alkenones (the upper solid line) and by alkenones in a coretop sample (the lower solid line), as described in text.

is based on a single culture experiment, it is typical of the isotopic difference observed between the biomass and extractable lipids of marine plankton [*Degens et al.*, 1968]. Revisions of this value are, therefore, not likely to be large. Any that were made would have the effect of repartitioning the total isotopic fractionation (i.e., between the separate processes of C-fixation and biosynthesis) but, for the reasons noted above, would not affect estimates of PCO_2.

ε_p: the isotopic fractionation accompanying photosynthetic fixation of carbon.

$$\varepsilon_p \equiv (\alpha_p - 1)10^3 = [(\delta_d + 1000)/(\delta_p + 1000) - 1]10^3 \quad (4)$$

This definition of ε_p reverses the sign (from negative to positive values) from earlier work [*McCabe*, 1985; *Popp et al.*, 1989; *Jasper and Hayes*, 1990]. It is now consistent with the plant physiological literature and provides a more intuitive measure in which larger values correspond to larger fractionations. Absolute values of ε_p are not significantly affected.

Determination of ε_p from δ_f and $\delta_{37:2}$. The equilibrium fractionation factor relating carbon isotopic compositions of HCO_3^- and CO_2(aq) has been measured by *Mook et al.* [1974]:

$$\varepsilon_{d/b} \equiv [(\delta_d + 1000)/(\delta_b + 1000) - 1]10^3 = 24.12 - 9866/T \quad (5)$$

where δ_b is the isotopic composition of dissolved bicarbonate and T is in kelvin. Similarly, *Morse and Mackenzie* [1990] have reviewed data relevant to equilibrium fractionation of carbon isotopes between dissolved bicarbonate and calcite and shown that

$$\varepsilon_{m/b} \equiv [(\delta_m + 1000)/(\delta_b + 1000) - 1]10^3 = 10.51 - 2980/T \quad (6)$$

Combination of (5) and (6) yields quantitative values for $\varepsilon_{m/d}$ (cf. equation (1)):

$$\varepsilon_{m/d} = -14.07 + 7050/T \quad (7)$$

Application of (1), (2) and (7) then allows calculation of δ_d from T and measured values of δ_f. Here temperatures derive from measurements of the alkenone-unsaturation parameter, U^K_{37}, in the same samples [*Lyle et al.*, 1992].

Calculation of oceanic PCO_2. Equilibrium PCO_2 values were calculated from values of c_e, ambient water temperatures [*Lyle et al.*, 1992], and Henry's law:

$$PCO_2 = c_e/K_H(T) \quad (8)$$

where $K_H(T)$ is the temperature-dependent Henry's law constant [*Weiss*, 1974].

Results and Discussion

Isotopic Records

The isotopic records of benthic and planktonic foraminifera, and those of the C_{37} alkadienones, and ε_p are presented here. The relationship between ε_p and [CO_2(aq)] is then considered.

Benthic and planktonic foraminifera. Results of oxygen- and carbon-isotopic analyses of foraminiferal carbonates (Table 1, Figure 4) are similar to those in prior reports [*Mix et al.*, 1991; *Martinson et al.*, 1987; *Shackleton et al.*, 1983] and the stratigraphy and application of the

Table 1. Foraminiferal Data From MANOP Site C (W8402-14GC)

Depth, cm	Age, kyr B.P.	*N. dutertrei*[a] $\delta^{13}C$	*N. dutertrei*[a] $\delta^{18}O$	*C. wuellerstorfii*[a] $\delta^{13}C$	*C. wuellerstorfii*[a] $\delta^{18}O$
1	0.6	1.34	0.12	--[b]	--[b]
3	1.7	1.33	0.36	2.50	0.28
7	3.9	1.36	0.39	2.62	0.13
18	6.1	1.33	0.49	2.71	0.09
23	10.0	1.16	0.87	3.12	-0.12
28	12.3	1.27	0.86	3.40	-0.17
30	14.7	1.27	0.71	4.08	-0.38
33	17.0	1.43	1.07	4.23	-0.38
38	19.4	1.27	1.06	3.93	-0.30
43	21.7	1.48	0.74	4.01	-0.19
48	24.0	1.55	0.85	4.11	-0.22
53	26.9	1.48	0.76	3.80	-0.10
58	29.9	1.47	0.54	3.71	-0.01
63	32.8	1.53	0.52	3.63	-0.03
68	35.7	1.48	0.69	3.63	-0.07
73	38.6	1.68	0.31	3.56	0.00
78	41.5	1.62	0.44	3.47	0.01
83	20.5	1.65	0.32	--[b]	--[b]
88	47.4	1.41	0.57	3.72	0.10
93	50.3	1.50	0.28	3.59	0.01
98	53.2	1.65	0.15	3.51	-0.12
103	56.2	1.44	0.43	3.59	-0.10
108	59.1	1.39	0.45	3.47	-0.33
113	62.0	1.33	0.45	3.56	-0.45
118	65.0	1.30	0.54	3.75	-0.26
123	68.8	1.36	0.44	3.75	-0.15
128	72.5	1.64	0.01	3.58	-0.12
133	76.3	1.72	-0.41	3.27	-0.01
138	80.0	1.44	-0.15	3.28	0.06
143	83.9	1.71	-0.36	3.24	0.07
148	87.0	1.69	-0.27	3.15	-0.13
151	91.4	1.78	-0.44	3.11	-0.04
153	93.5	1.73	-0.35	3.19	-0.04
158	99.0	1.57	-0.24	2.95	-0.00
161	102.3	1.70	-0.55	3.29	0.04
163	111.3	1.52	-0.34	3.20	-0.12
166	117.8	1.63	-0.65	2.87	-0.08
168	120.7	1.24	-0.57	2.60	0.17
170	122.2	1.23	-0.56	3.10	-0.12
173	124.3	1.26	-0.57	2.86	-0.08
176	126.5	1.06	-0.06	3.21	-0.50
178	128.0	1.29	-0.36	3.23	-0.40
180	129.4	1.14	0.35	3.65	-0.48
183	131.5	1.28	0.17	3.63	-0.50
188	135.0	1.41	0.17	3.68	-0.35
191	136.9	1.50	0.19	3.37	-0.69
198	141.4	1.49	0.06	3.73	-0.50
203	144.6	1.54	0.10	3.71	-0.40
208	147.8	1.41	0.24	3.67	-0.54
213	151.0	1.42	0.25	3.64	-0.58
221	158.0	1.31	0.22	3.26	-0.61
226	162.3	--[a]	--[a]	3.38	-0.61
231	166.6	1.52	-0.19	3.32	-0.56
236	171.0	1.49	-0.37	3.13	-0.49
241	174.0	1.14	-0.06	3.08	-0.58
246	177.0	1.36	-0.17	3.21	-0.56
256	183.0	1.63	-0.27	3.73	-0.45
261	194.0	1.50	0.08	3.28	-0.22
266	199.0	1.65	-0.22	3.56	-0.38

Table 1. (continued)

Depth, cm	Age, kyr B.P.	*N. dutertrei*[a] $\delta^{13}C$	*N. dutertrei*[a] $\delta^{18}O$	*C. wuellerstorfii*[a] $\delta^{13}C$	*C. wuellerstorfii*[a] $\delta^{18}O$
271	204.0	1.59	-0.17	3.16	-0.13
276	209.0	1.70	-0.42	2.78	-0.09
281	214.0	1.59	-0.37	2.78	0.05
286	220.0	1.35	-0.38	3.25	-0.34
291	224.0	1.36	-0.23	3.28	-0.30
296	228.0	1.30	-0.15	3.52	-0.35
301	231.3	1.30	-0.16	3.37	-0.31
306	234.7	1.47	-0.52	3.10	-0.13
311	238.0	1.19	-0.24	3.08	-0.15
316	241.3	1.34	-0.12	3.27	-0.33
321	244.7	1.39	-0.09	3.82	-0.60
326	253.2	1.36	0.21	3.70	-0.48
331	257.5	1.53	-0.09	3.83	-0.62

[a]Precisions for $\delta^{18}O$ and $\delta^{13}C$ results are both ±0.03‰, as described in the samples and methods section in text.
[b]Not available.

timescale is straightforward (Table 2). The planktonic $\delta^{18}O$ record appears anomalous because values from the core top to ~40 kyr are 0.5 to 1.0‰ higher than those of the previous glacial-to-interglacial episode. Benthic foraminifera are not similarly enriched in ^{18}O. This suggests either anomalously low temperatures in the upper ocean (which are not indicated by U^K_{37} temperature estimates) or deepening of the mean calcification depth for *N. dutertrei* during the last 40 kyr. As expected if the calcification depth had increased, the relatively high $\delta^{18}O$ values in the upper part of the core are accompanied by slightly reduced (< 0.3‰) $\delta^{13}C$ differences between the benthic and planktonic foraminifera. If the high $\delta^{18}O$ values in *N. dutertrei* near the core top are taken as implying calcification in deeper, colder water, annual mean temperature and salinity data for this site [*Levitus*, 1982] together with $\delta^{18}O$-salinity relationships [*Craig and Gordon*, 1965] suggest that the change in depth of calcification amounted to ~30 m. This shift would be reflected by $\delta^{13}C$ changes in the ambient water column of 0.1 to 0.3‰ [*Quay et al.*, 1992]. Accordingly, estimated values of δ_d might be low by that amount if the depth of growth of the Prymnesiophytes did not shift in parallel with the calcification depth of *N. dutertrei*. Such an error is, however, smaller than the typical standard deviation of the measurements of $\delta^{13}C$ in C_{37} alkadienones (~ 0.3‰) and thus would not significantly modify the estimates of paleoceanic PCO_2.

The ^{13}C in primary organic carbon, photosynthetic fractionation. Results of isotopic analyses of C_{37} alkadienones in 65 samples spanning 252 kyr show values of $\delta_{37:2}$ spanning 3.1‰, from -23.5 to -26.6‰ vs. PDB (Table 3). The calculations outlined in equations 1-7, together with δ_f values interpolated linearly with age from the planktonic record, allow construction of a record of changes in ε_p graphically summarized in Figure 5a (see also Table 3). At MANOP site C, ε_p varies over 3.3‰, ranging from 11.2 to 14.5‰.

For comparison, the glacial-to-interglacial variation in ε_p values is 5.3‰ in the Pigmy Basin in the northern Gulf of Mexico [*Jasper and Hayes*, 1990]. Not only is the amplitude of variation in ε_p smaller in the equatorial Pacific record, its core top value (13.9‰) is also smaller than that in the Gulf of Mexico (15.2‰). Although the pattern of variation in ε_p in both localities is consistent with the widely observed relationship in which decreased isotopic fractionation is associated with decreased concentrations of dissolved CO_2 (see discussion and citations in introduction), the observed differences raise questions about the nature of the ε_p-c_e relationship. At present, for example, since concentrations of dissolved CO_2 in the equatorial Pacific (where surface waters are a significant source of CO_2 to the atmosphere) are certainly higher than in the Gulf of Mexico, why is ε_p lower in the Pacific?

Relationships Between ε_p and c_e

The first expression explicitly relating ε_p and c_e was provided by *Farquhar et al.* [1982]:

$$\varepsilon_p = \varepsilon_t + (c_i/c_e)(\varepsilon_f - \varepsilon_t) \quad (9)$$

where ε_t and ε_f are respectively the isotope effects associated with the transport of CO_2 from the environment of the photosynthetic cell to the site of fixation and with intracellular fixation of CO_2 and c_i is the internal concentration of dissolved CO_2. More recently, alternative functional forms for the ε_p-c_e relationship and additional factors affecting ε_p have been discussed in several reports. *Rau et al.* [1992] indicated specifically that the difference between extracellular and intracellular concentrations of dissolved CO_2; that is the concentration gradient, $c_e - c_i$, must be a key factor. *Francois et al.* [1993] extended this conclusion by relating $c_e - c_i$ to growth rate and membrane permeability. Summarizing those findings, *Hayes* [1993] suggested an expression of the form:

$$\varepsilon_p = \varepsilon_f + (\gamma/c_e)(\varepsilon_t - \varepsilon_f) \quad (10)$$

where γ is the concentration gradient, $c_e - c_i$. This expression is expected to pertain only to organisms in which CO_2 reaches the site of fixation solely by passive diffusion, a limitation that arises because additional factors come into play when algae actively transport inorganic carbon into their cells (compare (17) and (19) of *Hayes* [1993] and see discussion by *Francois et al.* [1993]). Available evidence [*Raven and Johnston*, 1991] indicates that the Prymnesiophyte algae meet this requirement. Provided that carbon demand (γ) is constant, relationships between ε_p and c_e are then expected to fit expressions of the following form:

$$\varepsilon_p = a + b/c_e \quad (11)$$

where a and b are constants. Depending on the characteristics of the C-fixing community, a will represent ε_f or the sum of isotope effects associated with fixation and active uptake of inorganic carbon and b will represent either $\gamma(\varepsilon_t - \varepsilon_f)$ or a coefficient related to the "leakiness" of cells that actively assimilate inorganic carbon [*Hayes*, 1993]. Given this background, it is of interest to determine whether natural data sets yield ε_p-c_e relationships conforming to (11).

Four different sets of paired ε_p and c_e values are currently available. First, reconsideration of the Pigmy Basin ε_p-c_e data [*Jasper and Hayes*, 1990] in terms of the functional form of

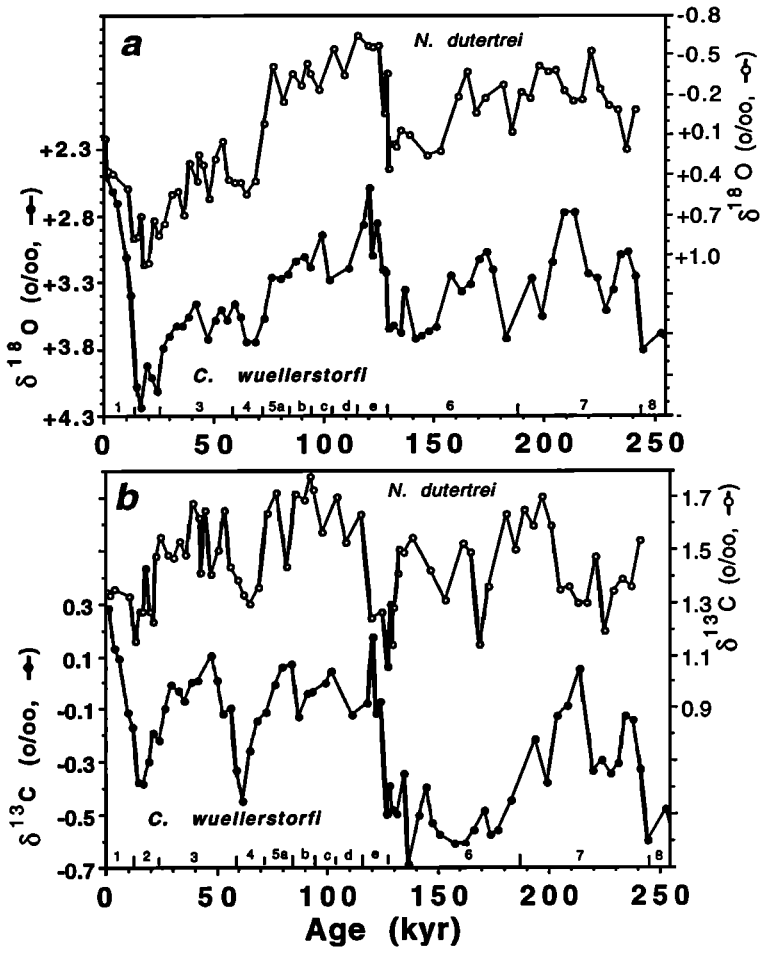

Figure 4. Time series records of (a) $\delta^{18}O$ and (b) $\delta^{13}C$ of the benthic foraminiferan *C. wuellerstorfii* and of the planktonic foraminiferan *N. dutertrei* from MANOP site C, sediment core W8402A 14GC. Oxygen isotope stage boundaries were determined by application of the SPECMAP chronological method [*Imbrie et al.*, 1984] to the $\delta^{18}O$-*C. wuellerstorfii* record and are identified along the abscissa in the following figures.

(11) yields a significant correlation (r^2 = 0.91, n = 8), a = 29.2 ± 2.7‰, and b = -109 ± 14 ‰ μM (indicated uncertainties are ± 1σ). A set of eight data points (for sedimentary stratigraphic intervals which correspond to Vostok pCO_2 ranges < 20 μatm) was used to relate the Gulf of Mexico (Deep Sea Drilling Project (DSDP) 619) record of ε_p values to equilibrium c_e values calculated from the Vostok ice core CO_2 record [*Barnola et al.*, 1987]. Here (Figure 6), that relationship has been updated by incorporation of the effects of the glacial-interglacial temperature change (23°-25°C, ^{18}O-derived temperatures discussed by *Jasper and Gagosian* [1989]), which has a small effect on both $\varepsilon_{m/d}$ and c_e. It is possible that air-sea equilibrium did not prevail or that, even if it did, the concentration of dissolved CO_2 at the depth of alkenone synthesis differed from the surface equilibrium value. The quality of the correlation and the observation that the intercept does not differ significantly from the ε_f value found in previous, plant-physiological studies [*Farquhar and Richards*, 1984] however, suggest that actual values of c_e were proportional to the calculated equilibrium values, that values of γ were roughly constant in this setting, and that the functional form of (11) is appropriate. Notably, the Pigmy Basin ε_p record, like that from the MANOP site, is based on alkenones and thus refers specifically to Prymnesiophyte algae.

Second, three remaining sets of ε_p, c_e pairs are based on analyses of POC in modern water columns. All derive from highly productive localities, specifically, the site of the North Atlantic Bloom Experiment (47°N, 20°W) [*Rau et al.* 1992], the chlorophyll maximum of the Santa Monica Basin (*D. Hollander et al.*, personal communication, 1993), and the Indian Ocean south of the Subtropical Convergence [*Francois et al.*, 1993]. For reasons discussed below, data from the relatively oligotrophic waters north of the Subtropical Convergence (also reported by *Francois et al.* [1993]) have been excluded from the regression yielding the line shown in Figure 6 (r^2 = 0.94, n = 34, a = 25.2 ± 0.5‰, b = -164 ± 7‰ μM). The observation of a good linear correlation again indicates the appropriateness of the functional form of (11), and the value found for a is again close to 27‰, the value of ε_f expected on the basis of biochemical evidence [*Farquhar and Richards*, 1984]. Because virtually all models of isotopic fractionation predict that ε_p will approach ε_f at high concentrations of dissolved CO_2 ($1/c_e \rightarrow 0$), it is likely that

Table 2. Age Model For MANOP Site C

Depth cm	Age kyr B.P.	Depth cm	Age kyr B.P.
0	0	178	128
18	10	188	135
48	24	213	151
108	59	236	171
118	65	256	183
138	80	261	194
147	87	281	216
158	99	296	228
161	107	311	238
167	120	321	249

assignment of a = -27‰ will prove robust. It remains to determine why the slopes of the ε_p-c_e relationships differ. This point is of particular significance because it may explain the differing ε_p ranges (3.1 versus 5.3‰) observed in the MANOP and Pigmy Basin records.

As indicated by the discussion leading to (11), the slope of the ε_p versus $1/c_e$ line will be controlled by magnitudes of isotope effects and by physiological factors that affect γ. Because the lines in Figure 6 have closely similar intercepts ($\approx \varepsilon_f$) and because ε_t is small and certain to be common to all systems, the observed variations in the slope [$\approx \gamma(\varepsilon_t - \varepsilon_f)$] are probably due to variations in γ. Significantly, (1) *Francois et al.* [1993] have noted that nutrient levels could affect growth rates and thus values of γ, and (2) nutrient levels in the comparatively oligotrophic Gulf of Mexico are very likely lower than in the highly productive localities represented by the steeper line. Moreover, values of ε_p for POC collected in the oligotrophic waters north of the Subtropical Convergence [*Francois et al.*, 1993] tend to bridge the gap between the lines, with nutrient levels approaching those in the Gulf of Mexico. As noted above, these points were omitted from the regression yielding the steeper line. Here, if it is accepted that membrane permeability is not likely to have differed greatly between Prymnesiophytes in the Gulf of Mexico and those in the equatorial Pacific, nutrient-related differences in growth

Table 3. Alkenone, ϵ_p and CO_2 Data From MANOP Site C (W8402-14GC)

Depth, cm	Age, kyr B.P.	$U^{K'}_{37}$-T[a], °C	$\delta^{13}C_{37:2}$[b], ‰ PDB	ε_p[c], ‰	CO_2 (aq)[d], µM	PCO_2[e], µatm
1.5	0.8	27.0	-26.1±0.3	13.9±0.3	9.92	353
7.5	4.2	27.1	-25.4±0.4	13.2±0.4	9.41	336
12.5	6.9	26.5	-24.3±0.4[f]	12.0±0.4	8.41	296
16.5	9.2	26.7	--[g]	--	--	--
19.5	10.7	26.6	-24.3±0.4	12.0±0.4	8.66	306
22.5	12.1	26.7	-24.6±0.4	12.1±0.4	8.66	305
25.5	13.5	26.7	-24.5±0.4	12.1±0.4	8.72	308
28.5	14.9	26.7	--	--	--	--
31.5	16.3	26.4	-25.3±0.4[f]	13.1±0.4	9.68	342
34.5	17.7	26.0	-24.6±0.3	12.3±0.3	8.86	311
37.5	19.1	25.8	-24.6±0.4[f]	12.3±0.4	8.75	304
44.5	22.4	25.6	-25.6±0.4	13.4±0.4	9.57	331
45.5	22.9	26.3	--	--	--	--
50.5	25.5	25.3	-25.4±0.4[f]	13.2±0.4	9.49	332
55.5	28.4	25.3	-24.8±0.3	12.5±0.3		
60.5	31.3	25.0	-24.5±0.2	12.3±0.3	8.84	301
64.5	33.6	25.3	-25.1±0.4	12.9±0.4	10.10	344
70.5	37.2	24.7	-25.5±0.4	13.4±0.4	9.55	323
75.5	40.1	25.6	--	--	--	--
80.5	43.0	25.6	--	--	--	--
85.5	45.9	25.6	--	--	--	--
90.5	48.9	25.7	-24.3±0.3	12.1±0.3	8.73	300
92.5	50.0	25.8	--	--	--	--
95.5	51.8	26.2	--	--	--	--
100.5	54.7	25.9	-24.4±0.3	12.3±0.3	8.87	309
101.5	55.3	25.8	-24.6±0.4	12.4±0.4	8.93	309
105.0	57.3	25.5	--	--	--	--
105.5	57.6	25.6	-25.6±0.4	13.4±0.4	9.53	327
110.5	60.5	26.2	--	--	--	--
111.5	61.1	26.0	-25.4±0.3[f]	13.1±0.3	9.39	328
115.5	63.5	26.2	-25.1±0.3	12.8±0.3	9.16	318
116.5	64.1	26.1	-24.4±0.4[f]	12.0±0.4	8.67	303
120.0	66.5	25.0	-24.9±0.3[f]	12.4±0.3	8.99	313
122.5	68.4	25.7	-24.3±0.3	12.0±0.3	8.63	292
125.0	70.3	25.9	-23.9±0.3	11.7±0.3	8.22	283
128.5	72.9	25.2	-25.7±0.4	13.7±0.4	9.78	339
130.8	74.6	25.6	-25.3±0.4	13.3±0.4	9.46	322

Table 3. (continued)

Depth, cm	Age, kyr B.P.	$U^{K'}_{37}$-T[a], °C	$\delta^{13}C_{37:2}$[b], ‰ PDB	ε_p[c], ‰	CO_2 (aq)[d], µM	PCO_2[e], µatm
132.3	75.8	26.0	-24.9±0.3	12.9±0.3	8.73	300
136.5	78.9	25.6	-25.2±0.4	13.0±0.4	9.33	324
139.5	81.2	25.7	-26.6±0.4[f]	14.6±0.4	10.44	359
141.5	82.7	26.8	--	--	--	--
144.5	85.0	25.4	--	--	--	--
145.5	85.8	26.2	-26.4±0.4[f]	14.5±0.4	10.47	371
151.5	91.9	25.9	-25.7±0.4	13.9±0.4	9.90	339
155.5	96.3	26.2	--	--	--	--
161.5	108.1	26.5	-25.1±0.4	13.1±0.4	9.05	314
167.5	120.4	25.6	--	--	--	--
171.0	122.9	27.2	-25.1±0.4	12.8±0.4	9.38	330
175.5	126.2	27.4				
180.5	129.7	26.8	-25.9±0.4	13.6±0.4	9.67	348
186.5	133.9	26.5	--	--	--	--
190.5	136.6	25.6	--	--	--	--
195.5	139.8	26.5	-25.2±0.4	13.1±0.4	9.33	321
201.5	143.7	25.3	-24.8±0.4	12.7±0.4	8.90	313
202.5	144.3	26.0	-25.1±0.4	13.0±0.4	9.28	316
205.5	146.2	25.6	-23.5±0.4	11.2±0.4	8.26	287
206.5	146.9	26.1	--	--	--	--
211.5	150.1	25.9	-24.1±0.3	11.8±0.3	8.57	298
214.5	152.3	25.8	-24.2±0.3	12.0±0.3	8.65	299
215.5	153.2	26.5	--	--	--	--
218.5	155.8	25.6	-24.4±0.3	12.0±0.3	8.70	306
223.5	160.1	25.8	-24.3±0.2	12.0±0.3	8.67	298
224.5	161.0	25.3	-24.6±0.3[f]	12.2±0.3	8.82	305
229.5	165.3	25.6	-24.5±0.3	12.3±0.3	8.82	301
230.8	166.5	25.6	-25.3±0.3	13.2±0.3	9.40	323
235.0	170.1	25.3	-24.9±0.4	12.7±0.4	9.14	314
236.5	171.3	25.7	--	--	--	--
240.5	173.7	26.2	-24.5±0.2[f]	12.0±0.3	8.66	298
244.3	176.0	26.3	-25.9±0.3[f]	13.6±0.3	9.70	339
245.5	176.7	25.6	-25.2±0.3	12.9±0.3	9.24	323
250.5	179.7	25.6	-24.9±0.3[f]	12.7±0.3	9.08	312
254.3	182.0	25.8	-24.2±0.3	12.1±0.3	8.72	300
256.5	183.9	25.9	-24.3±0.3[f]	12.3±0.3	8.81	304
261.5	194.5	25.9	-25.4±0.3[f]	13.3±0.3	8.42	292
265.5	198.5	26.2	-25.6±0.4	13.7±0.4	9.75	338
267.0	200.0	25.9	-24.1±0.3	12.1±0.3	8.75	305
270.5	203.5	25.3	-25.2±0.3	13.1±0.3	9.41	326
275.5	208.5	26.6	-25.8±0.3	13.9±0.3	10.12	357
280.5	213.5	26.2	-25.8±0.4	13.8±0.4	9.86	344
285.5	219.6	26.6	-26.5±0.3[f]	14.3±0.3	10.21	356
290.5	223.6	26.8	-25.8±0.4	13.7±0.4	9.73	343
295.5	227.6	26.7	-25.7±0.4[f]	13.4±0.4	9.58	339
301.0	231.3	26.2	-26.2±0.3[f]	13.9±0.3	9.98	353
305.5	234.3	26.5	-26.5±0.4	14.4±0.4	7.77	271
310.5	237.7	26.8	--	--	--	--
316.0	243.5	26.6	--	--	--	--
321.0	249.0	25.4	-25.9±0.4	13.6±0.4	9.77	344
325.5	252.8	26.3	-24.9±0.4[f]	12.7±0.4	9.02	308

[a] $U^{K'}_{37} = [C_{37:2}]/([C_{37:2}] + [C_{37:3}])$, where $C_{37:2} = C_{37}$ alkadienone and $C_{37:3} = C_{37}$ alkatrienone, as defined by *Brassell et al.* [1986] and calibrated by *Prahl and Wakeham* [1987]. These are the numerical $U^{K'}_{37}$ data from which graphs of *Lyle et al.* [1992] are generated.

[b] The $\delta^{13}C$ value of the C_{37} alkadienone (heptatriaconta-15,22-dien-2-one) and pooled (1σ) estimates of standard deviation ($1\sigma = 0.43/\sqrt{n}$, where n is the number of replicate analyses).

[c] Values of ε_p ±1σ standard deviations from $\delta_{37:2}$ and $\delta_{N.\ dutertrei}$, as described in text.

[d] calculated using (11) with a = 27‰ and b = -130‰ µM

[e] calculated using estimated c_e, $U^{K'}_{37}$ T, and (8).

[f] Samples saponified to remove co-eluting alkenoates. (See samples and methods section in text.)

[g] Not available typically because of insufficent (<10 nmol) $C_{37:2}$alkenone-C.

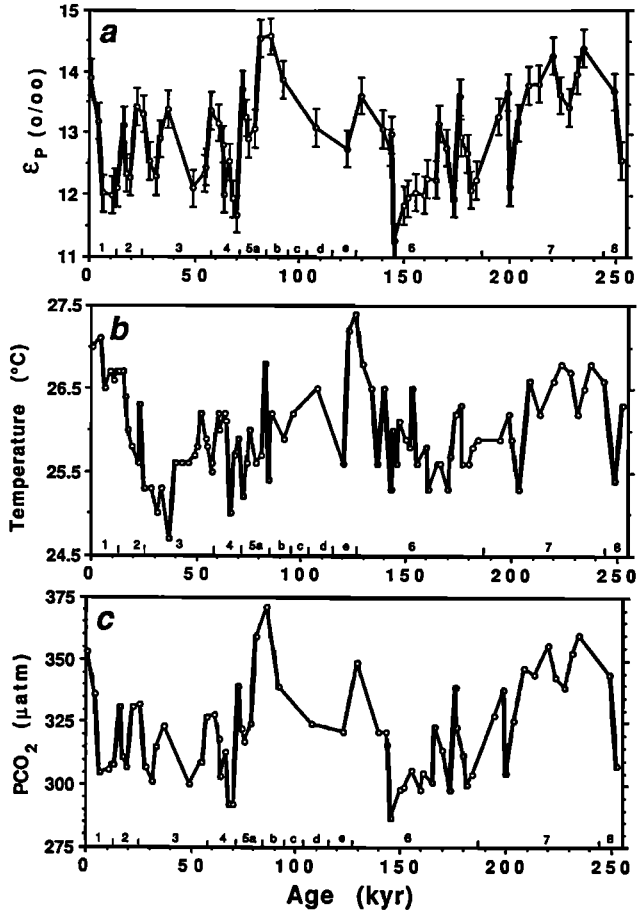

Figure 5. Time series records of (a) ε_p, calculated using (4), with 1σ error bars reflecting the uncertainties in δ_d and δ_p, assuming that standard deviations in these parameters are equal to those in δ_f and $\delta_{37:2}$, respectively; (b) temperature of Prymnesiophyte growth, calculated using the relationship found by *Lyle et al.* [1992]; and (c) PCO_2 of water in which the Prymnesiophytes grew, calculated using (8) and c_e derived from (11) with a = 27‰ and b = -130‰ µ*M*.

rate (taken as proportional to γ, carbon demand) are by default the most likely cause of the different ε_p ranges and different core top fractionations found in the Pigmy Basin and MANOP cores. This view is supported strongly by new measurements of ε_p in equatorial Pacific waters [*Fluegge*, 1994] which show that ε_p varies inversely with the strength of upwelling (as judged from sea surface temperatures) and thus with nutrient levels. If it is assumed that the waters above the MANOP core site have been consistently affected by upwelling (a point considered below), the slope of the applicable ε_p versus $1/c_e$ line can be estimated by accepting a $1/c_e = 0$ intercept of 27‰ and then adjusting the line so that it passes through ε_p, $1/c_e$ points representative of present conditions.

There are two independent approaches to this problem. First, there are new, alkenone-based observations of ε_p in present-day equatorial Pacific waters [*Fluegge*, 1994] for which c_e values are known (*C. Goyet*, personal communication, 1993). Second, there is the MANOP-C core top ε_p value, which should relate to pre-industrial CO_2 levels. From the first source (2°-5° N and S) [*Fluegge*, 1994] we obtain the c_e, ε_p points marked by open circles on the graph inset in Figure 3. The upper solid line on this graph extends from an ε_p intercept of 27‰ through the centroid of these points and yields b = -126‰ µ*M*. To use the core top data, an estimate of the pre-industrial c_e is required. Given a pre-industrial atmospheric pCO_2 of 280 µatm [*Neftel et al.*, 1985], it would be possible to calculate the equilibrium c_e for a given sea surface temperature. However, it is known that equatorial Pacific waters are not in equilibrium with the atmosphere and it is necessary first to obtain an estimate for the pre-industrial ΔpCO_2 (surface waters versus atmosphere). The pre-industrial disequilibrium must have been greater than that at present, since anthropogenic inputs to the atmosphere have the effect of decreasing the disequilibrium. To estimate the ΔpCO_2 that would be observed in the absence of anthropogenic inputs, we estimate that waters upwelling in the equatorial Pacific at present have an age (since last exposure to the atmosphere) of approximately 30 years. During that interval, atmospheric pCO_2 has increased by 35 µatm [*Keeling et al.*, 1989]. The presently observed ΔpCO_2 (50 µatm) [*Murray et al.*, 1993] is thus 35 µatm smaller than that which would be observed without anthropogenic inputs. Estimating, then, a pre-industrial ΔpCO_2 of 50 + 35 = 85 µatm, we compute c_e = 10.26 µ*M* at a sea surface temperature of 27°. Given the core top fractionation of 13.9‰, we find b = -134‰ µ*M*. As shown in Figure 3, the lower solid line, which represents this value of b, passes just below the cluster of points derived from the

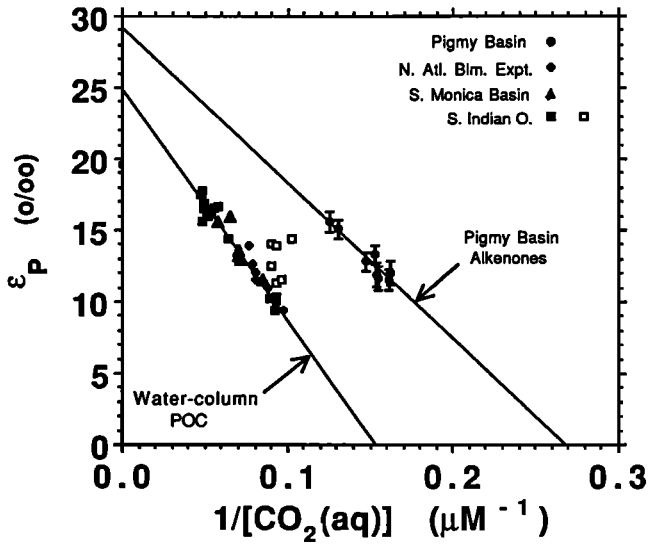

Figure 6. Calibrations of ε_p versus c_e based on Pigmy Basin alkenones and on water-column particulate organic carbon. Molecular isotopic (C_{37} alkenone) and planktonic foraminiferal (*G. ruber*) results were used for the calibration line for Pigmy Basin sedimentary components. Water column POC calibrations are based on $\delta^{13}C$ and c_e from the North Atlantic Bloom Experiment [*Rau et al.*, 1992], the Santa Monica Basin [*Wakeham et al.*, 1993], and the southern Indian Ocean [*Francois et al.*, 1993]. Only the oligotrophic (with less than measurable nitrate) water-column data are shown by open squares.

modern water column. Notably, the first of these lines is based on material collected at the sea surface and the second on sedimentary debris. The estimated ε_p versus $1/c_e$ lines are not coincident, but their small difference suggests that effects associated with sedimentation and preservation are small. Nominal estimates of c_e can be based on the heavy, dotted line ($\varepsilon_p = 27 - 130/c_e$) placed halfway between these lines.

Uncertainties associated with the reconstruction of PCO_2. If this line is now used to estimate concentrations of dissolved CO_2 based on values of ε_p, at least three categories of uncertainty are involved. There are, first, those which are amenable to statistical assessment and which involve propagation of uncertainties associated with the analytical measurements themselves. In terms of an ε_p versus $1/c_e$ plot these lead straightforwardly to error bars parallel to the ε_p axis. Establishment of uncertainties for estimates of c_e, however, requires assessment of uncertainties associated with placement of the line relating ε_p and $1/c_e$. As implied by the foregoing discussion, these are not amenable to statistical treatment and relate instead to the choice and realism of the calibration data themselves (e.g., Is 280 µatm the best pCO_2 value to pair with the core top ε_p? Is the estimate of pre-industrial ΔpCO_2 accurate? Do fractionations based on analyses of materials from the water column merit consideration, given that the record is based entirely on sedimentary materials? [e.g., *Goericke and Fry*, 1994]). At present, the answers to these questions are not known. Useful consideration of variations in oceanic PCO_2 is, however, not precluded.

CO_2(aq) Concentration and Paleoceanic PCO_2 at MANOP Site C

Concentrations of dissolved CO_2 can be estimated using (11) with $a = 27‰$ and $b = 130‰$ µ*M* (i.e., the "nominal" line derived in the preceding discussion). Numerical values are reported in Table 3. Then, application of (8) together with the alkenone-based temperature record summarized in Fig. 5b yields the estimated PCO_2 record shown in Table 3 and Figure 5c. Estimated paleoceanic PCO_2 at this central equatorial Pacific site was higher during interglacial stages (~360 µatm) than during glacial stages (~280 µatm). The indicated range is ~80 µatm. Beyond a general correspondence with the atmospheric record [*Jouzel et al.*, 1993], however, there is notable decoupling from the general "sawtooth" pattern of climatic change. For example, the paleoceanic PCO_2 rise leads the ice core pCO_2 record by about 10 kyr near the stage 6-to-5 deglaciation. By contrast, the paleoceanic PCO_2 rise from the most recent (stage 2-to-1) deglaciation lags the ice core pCO_2 rise by about 5-15 kyr. A higher sampling frequency would be required to better constrain these leads and lags. It is also possible that our relatively coarse sampling interval masks potential high-frequency oscillations in paleoceanic PCO_2, or that local oceanographic effects such as upwelling and attendant changes in assemblages and biological CO_2 demand may cause paleoceanic PCO_2 variations that were decoupled from the paleoatmospheric pCO_2 record [*Rau et al.*, 1992; *Francois et al.*, 1993] during these deglacial transitions [*Pedersen*, 1983; *Lyle et al.*, 1988; *Pedersen et al.*, 1988, 1991]. For example, the high paleoceanic PCO_2 in late stage 6 might indicate relatively strong upwelling, without a proportional increase in primary productivity. In contrast, the relatively low paleoceanic PCO_2 of the stage 2-1 transition could reflect high export productivity relative to upwelling at that time [*Lyle et al.*, 1988].

Comparison of CO_2 records from MANOP Site C and the Vostok ice core. When the paleoceanic and paleoatmospheric records are compared, the record of estimated ΔpCO_2 values shown in Figure 7 is obtained. The record indicates that, as at present [e.g., *Tans et al.* 1990; *Murphy et al.* 1991], equatorial Pacific surface waters have been continuously supersaturated with CO_2 (equivalent to $60 \le \Delta pCO_2 \le 110$ µatm) throughout the last 255 kyr. Notably, however, estimated air-sea pCO_2 differences in glacial periods are systematically larger (~110 µatm) than those during interglacial periods (~60 µatm). If true, this would mean that this portion of the equatorial Pacific was an even stronger source of CO_2 to the atmosphere during glacial intervals than during interglacial periods.

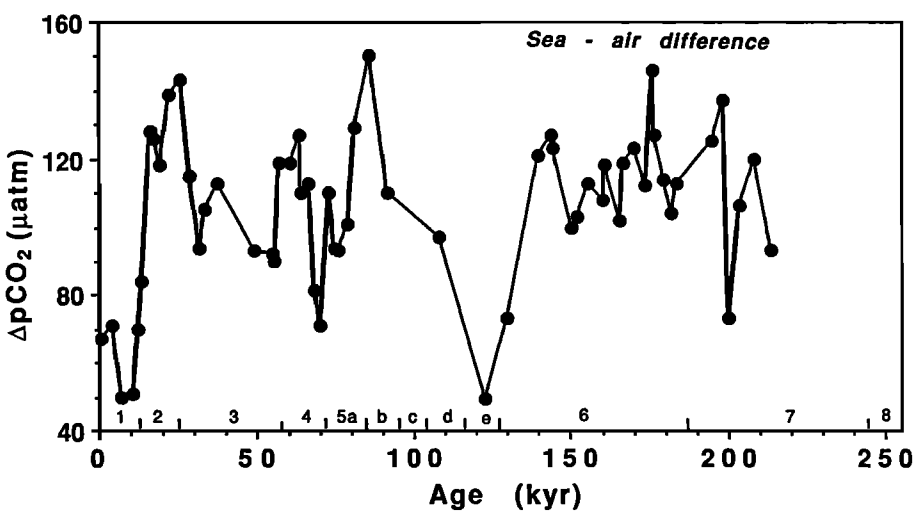

Figure 7. A record of ΔpCO_2 calculated from the estimates of paleoceanic PCO_2 shown in Figure 5c and the Vostok ice core pCO_2 record of *Jouzel et al.* [1993].

To explore this possibility, Figure 8 depicts an enlarged segment of a graph of ε_P versus $1/c_e$. The horizontal, dotted lines depict the average values of ε_P observed in the MANOP record under interglacial and glacial conditions. The vertical dotted line marks the glacial $1/c_e$ value required for constant ΔpCO_2 (60 μatm) at a glacial sea surface temperature of 25.5°C. The 60-μatm value is used here because it is that nominally found for the interglacial interval. If some other value were in fact correct, it would not have a large effect on the following discussion. The left-hand solid line represents the nominal relationship between ε_P and $1/c_e$ derived above and the dashed line at right represents a similarly derived relationship based on the Pigmy Basin record. Since we have observed that, during glacial intervals, average values of ε_P at this site declined only from 13.4 to 12.5‰, the graph indicates that, if ΔpCO_2 in fact remained constant, either (1) the ε_P-c_e relationship changed so that it was represented by the right-hand solid line, arbitrarily constructed so that it passes through the point representative of constant ΔpCO_2, or (2) the measured value of ε_P is in error by 3.3‰ (the amount required to reach the hypothetical $1/c_e$ value on the nominal line). In the first case, oceanographic conditions (presumably those regulating rates of algal growth) in the equatorial Pacific would have to have resembled those in the relatively oligotrophic Gulf of Mexico. It is, however, more likely that availability of nutrients was increased by wind-driven enhancement of mixing under glacial conditions [e.g., *Lyle et al.*, 1992]. Related changes in γ are then expected to steepen the slope depicted here rather than to displace it toward the Pigmy Basin line. Estimates of PCO_2 for glacial intervals might therefore be systematically higher than indicated in Figure 5c, but almost certainly not lower. Accordingly, the hypothesis that the observed, small change in ε_P actually represents constant ΔpCO_2 and changing γ rather than nearly constant c_e cannot be favored. In the alternative case the 31 independent measurements of ε_P during glacial intervals would have to be in error by more than 10σ. Since this is extremely unlikely, we reject the hypothesis that the small change in ε_P is actually due to mismeasurement.

The smoothed ΔpCO_2 record. The pattern of variations in ΔpCO_2 emerges with particular clarity when smoothed records are compared. The paleoceanic PCO_2 estimates and the Vostok paleoatmospheric pCO_2 record were both interpolated to 4-kyr intervals and smoothed with a 16-kyr-wide Gaussian convolution filter to facilitate calculation of differences, to minimize the effect of small correlation errors, and to emphasize major trends (Figure 9a). This filter effectively removes variability with a period of < 8 kyr but leaves the major glacial-interglacial signals intact [*Shackleton et al.*, 1992]. When fewer than two data points

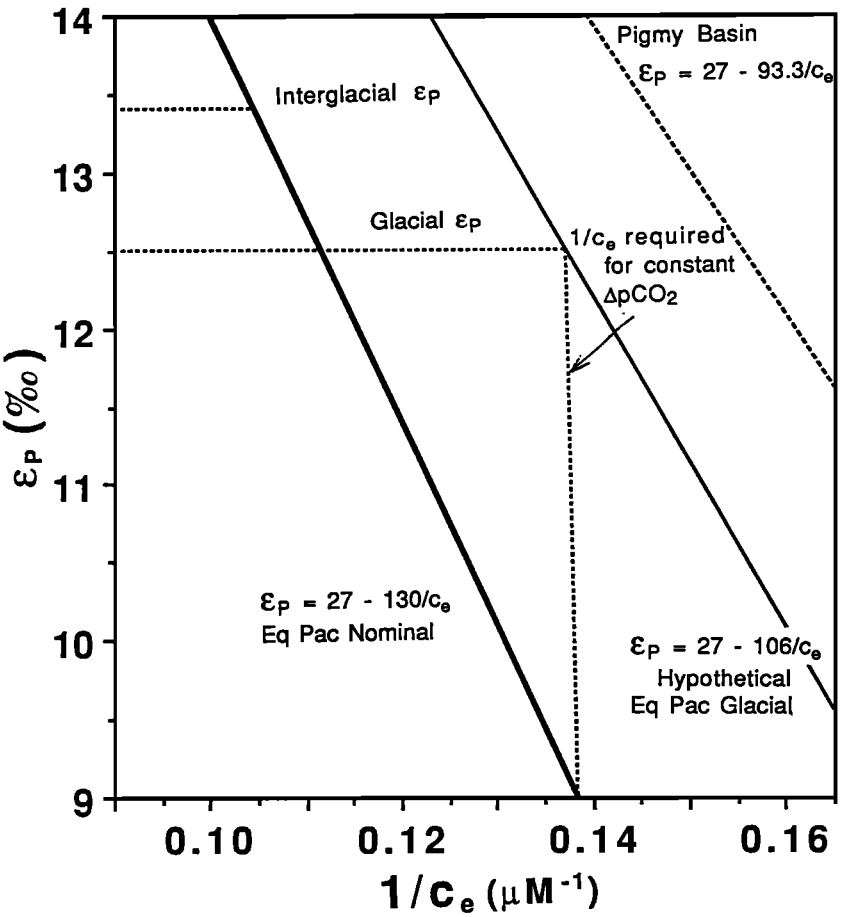

Figure 8. An expanded view of a graph like that shown in Figure 6. Equations of the lines are shown and their significance is discussed in the text.

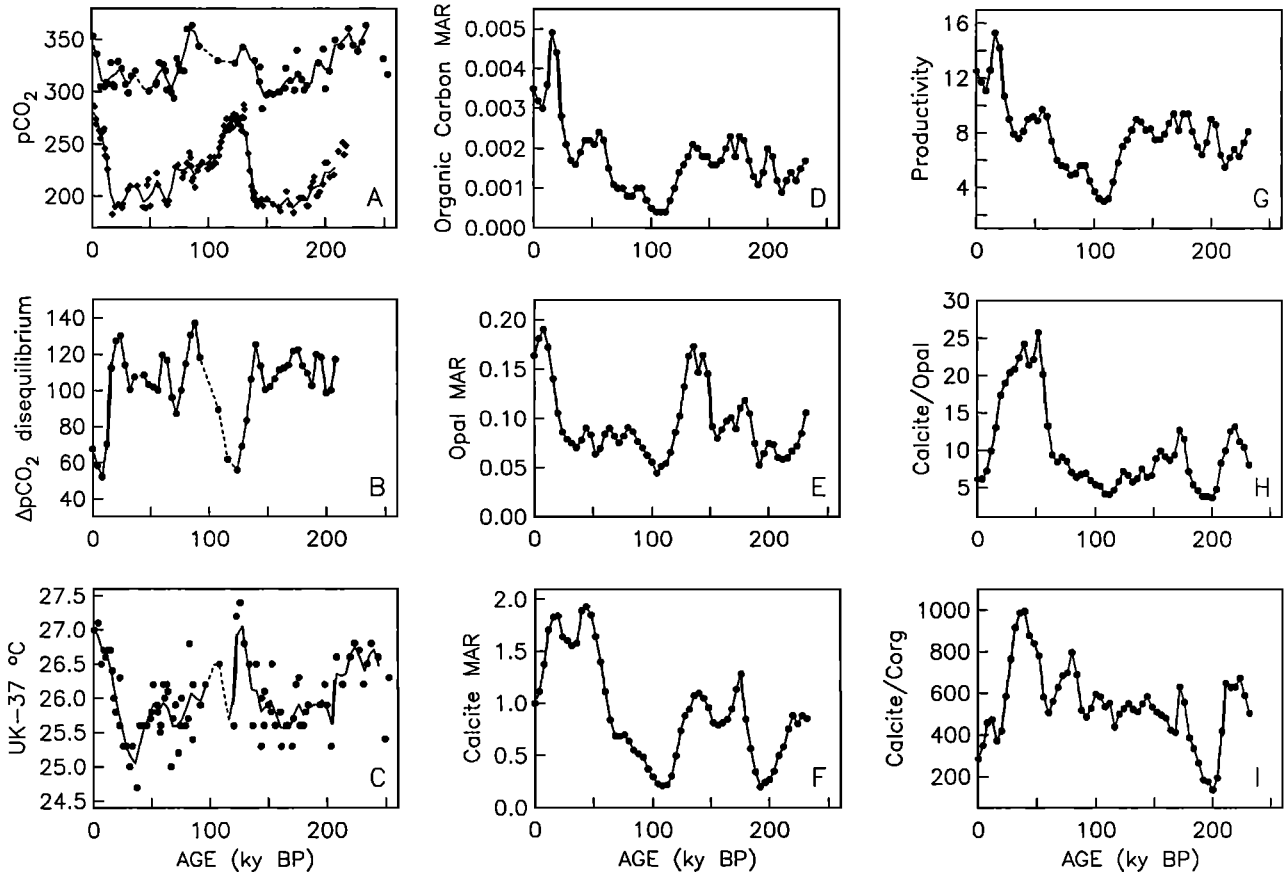

Figure 9. Time series records of (a) statistically smoothed PCO_2 (μatm) records reconstructed from MANOP site C and the Vostok ice core (as in Figure 6), (b) oceanic-atmospheric pCO_2 disequilibrium (ΔpCO_2, μatm) for this site, (c) $U_{37}^{K'}$-temperature, and mass accumulation rates (g/cm^2 kyr) of (d) total organic carbon, (e) opal, and (f) mineral carbonate. Also shown are (g) productivity index (in g/cm^2 kyr) [*Sarnthein et al.*, 1988], (h) calcite/opal ratio, and (i) calcite/C_{org} ratio.

occured within a 16-ka filter window, no data points were interpolated and the record was left blank. Calculated pCO_2 differences (ΔpCO_2) are shown in Figure 9b. Although this analysis may create spurious signals because of errors in correlation between the sediment and ice core records, the general features of the ΔpCO_2 record are likely robust. It is similar to the oxygen-isotope curve (Figure 4a) in that low values are observed during interglacial stages 1 and 5, intermediate values in stage 3, and high values during glacial stages 2, 4, and 6, suggesting a connection to glacial-interglacial climatic change.

Because fluxes are proportional to the concentration gradient, the observed variations would indicate that the sea-to-air flux of CO_2 during glacial periods was typically twice as high as that during interglacial periods. If so, production of the observed ice core record would require that sinks capable of overcompensating this flux existed elsewhere in the ocean-atmosphere system. In fact, *Keir* [1993] recently suggested that temperature-driven solubility pumping made the North Atlantic such a sink during glacial intervals. Moreover, using the ε_p-PCO_2 method described here, *Jasper et al.* [1993] found evidence that surface waters in that region were enriched in dissolved CO_2, an observation consistent with the possibility of subduction of particularly large quantities of CO_2. The difference is remarkable, because it indicates that, within this time frame, equatorial upwelling has worked against the atmospheric pCO_2 change and thus may be an important negative feedback in the global climate system.

The Relationship of PCO_2 and ΔPCO_2 to Other Paleochemical Variables

Records of $U_{37}^{K'}$-based temperature; of mass accumulation rates (MAR) of organic carbon, opaline silica, and calcite; of the Sarnthein export productivity index [*Sarnthein et al.*, 1988]; and of calcite/opal and calcite/C_{org} ratios [data from *Lyle et al.*, 1988, 1992, using the present modified timescale] are shown in Figures 9c-9i. As with the preceeding pCO_2 and ΔpCO_2 records (Figures 9a and 9b), all of these indices have been smoothed and interpolated. The resulting time series have been used to search for possible correlations with ΔpCO_2. Results are summarized in Table 4.

Correlations of ΔpCO_2 with $U_{37}^{K'}$ temperature and the opal mass accumulation rate are significant at the 99% confidence level. The simplest explanation of the correlation between ΔpCO_2 and temperature is that both respond to upwelling.

Table 4. Correlations Between ΔpCO_2 (W8402A-14GC-Vostok) And Other Biogeochemical Parameters In Core W8402A-14GC (n = 47)

Parameter	r
$U_{37}^{K'}$-temperature	-0.56*
Total C_{org} MAR	-0.10
Opal MAR	-0.41*
Calcite MAR	+0.02
Calcite/C_{org} ratio	+0.10
Calcite/Opal ratio	+0.21
Opal/C_{org} ratio	-0.19
Sarnthein export production	-0.09

Here r is the correlation coefficient based on smoothed interpolated time with all indices interpolated to 4 ka intervals with 16 ka Gaussian smoothing. Gaps in series left blank. The asterisk indicates correlation significantly different from zero at 99% level.

Higher glacial upwelling resulted in both lower temperatures [*Lyle et al.*, 1992] (also from W8402A-14GC) and higher ΔpCO_2 [*Tans et al.*, 1990; *Volk and Bacastow*, 1989]. The correlation of ΔpCO_2 with opal MAR is inverse; that is, ΔpCO_2 has been low when siliceous phytoplankton have been especially productive. There is a conceivable causal relationship, namely that fixation of CO_2 by diatoms decreased ΔpCO_2. Alternatively, factors controlling the delivery of CO_2 and of silica to these waters may be at least partly independent. The peaks in the rate of accumulation of opal must reflect peaks in the availability of silica, but concentrations of dissolved CO_2 might be responding to other factors. In the most extreme case the inverse correlation between ΔpCO_2 and opal MAR would reflect only variations in the $[CO_2(aq)]/[Si(OH)_4]$ ratio in the upwelling waters. The first alternative (i.e., drawdown of CO_2 by diatoms) could be preferred if the peaks in the accumulation rate of opal coincided with peaks in the accumulation rate of C_{org}, but they do not. Therefore, if the low ΔpCO_2 is attributed to drawdown, it must additionally be postulated that the resulting organic carbon was oxidized so completely that no record of it remains.

The weak positive correlation between ΔpCO_2 and carbonate/opal ratios could imply higher proportions of carbonate carbon in the biological carbon export during glacial time. Increasing the carbonate-to-organic carbon ratio in exported detritus would consume alkalinity and thus increase the $CO_2(aq)$ and PCO_2 of upper ocean water [*Broecker and Peng*, 1982, 1989; *Dymond and Lyle*, 1985]. Whether the high carbonate contents of glacial sediments in the equatorial Pacific reflect changes in preservation or in productivity has long been debated [*Arrhenius*, 1952; *Berger*, 1973; *Farrell and Prell*, 1989]. *Archer* [1991] modeled the effects of productivity and dissolution in the tropical Pacific and favored productivity as a major influence. Although he did not invoke a glacial increase in the calcite/total carbon rain ratio, this mechanism would be consistent with both his finding and our finding of relatively high glacial ΔpCO_2.

There are no significant correlations between ΔpCO_2 and the calcite/C_{org} or calcite/opal ratios. In the absence of the ΔpCO_2-opal correlation noted above, these observations would indicate that the composition of the phytoplanktonic community does not play an important role in determing oceanic CO_2 levels (however, differential preservation of the components may obscure the original compositional ratios). The Sarnthein paleoproductivity index [*Sarnthein et al.*, 1988], based on organic carbon and sedimentation rates, is also not significantly correlated with ΔpCO_2. On balance, these observations suggest that the most important controls on ΔpCO_2 were not biological.

Conclusions

We present here the first biomarker-specific isotopic reconstruction of upper oceanic PCO_2 in the late Pleistocene from the central equatorial Pacific, which is at present a large source of CO_2 to the atmosphere. A reassessment of the calibrations of bulk POC- and alkenone-based data for paleo-PCO_2 reconstruction supports the application of a hyperbolic model of the form $\varepsilon_p = a + b/c_e$ to quantify the relationship between photosynthetic isotope fractionation and concentrations of dissolved molecular CO_2. Comparison of the ~230-kyr Vostok ice core record of paleoatmospheric pCO_2 with the ~255-kyr, ε_p-based record of paleoceanic PCO_2 at MANOP site C indicates that the central equatorial Pacific was a continuous, climatically-linked source of CO_2 to the atmosphere over at least the ~230-kyr span of the ice core record. The air-sea difference in the partial pressure of CO_2 was typically larger in glacial periods (~110 μatm) than in interglacial periods (~60 μatm), indicating a significantly (~2 times) higher sea-to-air flux of CO_2 during glacial intervals. In order to maintain low glacial paleoatmospheric pCO_2 (~190 μatm) while there was apparently increased input of CO_2 from the equatorial Pacific, there must be larger sinks for CO_2 elsewhere in the glacial world. Studies of other critical regions of paleoceanic CO_2 exchange will be required to constrain the budget of CO_2 fluxes which combine to determine the paleoatmospheric pCO_2 which significantly contributes to the heat balance of the earth.

The central equatorial Pacific record of paleoceanic pCO_2 disequilibrium is significantly and inversely correlated with sea surface temperatures, which is consistent with higher upwelling causing both colder temperatures and higher oceanic ΔpCO_2 values.

Several uncertainties remain in the coupled use of planktonic foraminiferal and compound-specific $\delta^{13}C$ values to estimate past PCO_2. Present research indicates that the combination of plankton depth habitats, upwelling, primary productivity, and the chemical makeup of the local biota may all contribute to the carbon isotopic record of paleoceanic PCO_2. The constancy of offsets from $\delta^{13}C$ equilibrium in the foraminifera, and between bulk organic matter and biomarker $\delta^{13}C$ will require further investigation. The depth habitats and ecology of the alkenone producers are not well known, and the understanding of planktonic foraminiferal habitats is incomplete. Knowledge of the water column depths that are

monitored by the selected geochemical indices is essential to their use to infer paleoceanic CO_2 sources and sinks. Field and culture experiments to refine our understanding of processes responsible for fractionation of ^{13}C will help to constrain these uncertainties. The calibration of the equations translating ε_P into oceanic PCO_2 could be improved by analysis of samples in subtropical sites likely to be at pCO_2 equilibrium with the atmosphere throughout the late Quaternary. Although challenges remain, further application of the ε_P method should allow first-order reconstruction of concentrations of dissolved CO_2 in oceanic surface waters and will help to constrain locations and strengths of past oceanic sources and sinks for CO_2.

Acknowledgments. We thank the Oregon State University core repository (NSF OCE-9102881) for providing samples (MANOP site C core W8402A-14GC) for this research and J. Fong, A. Morey, K. Amthor, and K. S. Duke for scientific and technical contributions; M. Bacon for water column samples and C. Goyet for corresponding PCO_2 data (enumerated by *Fluegge* [1994]); G. Rau, B. Popp, R. Toggweiler, S. Anderssen, and E. A. Boyle for various scientific contributions to this study. NSF Ocean Sciences (Chemical Oceanography, NSF OCE 9216918) and NASA (NAGW-1940) support this research.

References

Archer, D. A., Equatorial Pacific calcite preservation cycles: Production or dissolution? *Paleoceanography, 6*, 561-572, 1991.

Arrhenius, G., Sediment cores from the east Pacific: Properties of sediments. *Rep. Swed. Deep Sea Exped., 1951-1952*, 1-227, 1952.

Arthur, M. A., W. E. Dean, and G. E. Claypool, Anomalous C-13 enrichment in modern marine organic carbon. *Nature, 315*, 216-218, 1985.

Barnola, J. M., D. Raynaud, Y. S. Korotkevich, and L. Lorius, Vostok ice core provides 160,000-year record of atmospheric CO_2, *Nature, 329*, 408-414, 1987.

Berger, W. H., Deep-sea carbonates: Pleistocene dissolution cycles. *J. Foraminiferal Res., 3*, 187-195, 1973.

Berger, W. H., Increase in carbon dioxide in the atmosphere during deglaciation: The coral reef hypothesis, *Naturwissen, 69*, 87-88, 1982.

Brassell, S.C., Eglinton, G., Marlowe, I.T., Pflaumann, U. and Sarnthein, M., Molecular stratigraphy: a new tool for climatic assessment. *Nature, 320*, 129-133, 1986.

Broecker, W. S., Glacial to interglacial changes in ocean chemistry. *Progr. Oceanogr., 11*, 151-197, 1982.

Broecker, W. S., and T.-H. Peng, *Tracers in the Sea*, 690 pp., Eldigio, Palisades, N. Y., 1982.

Broecker, W. S., and T.-H. Peng, The cause of glacial to interglacial atmospheric CO_2 change: A polar alkalinity hypothesis. *Global Biogeochem. Cycles, 3*, 215-239, 1989.

Craig, H., and L.I. Gordon, Deuterium and oxygen-18 variations in the ocean and marine atmosphere, in *Stable Isotopes in Oceanic Studies and Paleotemperatures*, edited by E. Tongiorgi, pp. 9-130, Consiglio Nazionale Delle Recerche, Laboratorie Di Geologica Nucleare, Pisa, Italy, 1965.

Degens, E. T., M. Behrendt, B. Gotthardt, and E. Reppmann, Metabolic fractionation of carbon isotopes in marine plankton, *Deep Sea Res., 15*, 11-20, 1968.

de Leeuw J. W., F. W. van de Meer , W. I. C. Rijpstra, and P. A. Schenck, On the occurrence and structural identification of long chain unsaturated ketones and hydrocarbons in sediments, in *Advances in Organic Geochemistry 1979*, edited by A. G. Douglas and J. R. Maxwell, pp. 211- 217, Pergamon, New York, 1980.

Dymond, J., and M. Lyle, Flux comparisons between sediments and sediment traps in the eastern equatorial Pacific: Implications for atmospheric CO_2 variations during the Pleistocene, *Limnol. Oceanogr., 30*, 699-712, 1985.

Emerson, S., C. Stump, P. M. Grootes, M. Stuiver, G. W. Farwell, and F. H. Schmidt, Estimates of degradable organic carbon in deep-sea surface sediments from ^{14}C concentrations, *Nature, 329*, 51-53, 1987.

Farquhar, G. D., and R. A. Richards, Isotopic composition of plant carbon correlates with water-use efficiency of wheat genotypes, *Aust. J. Plant Physiol., 11*, 539-552, 1984.

Farquhar, G. D., M. H. O'Leary, and J. A. Berry, On the relationship between carbon isotope discrimination and the intercellular carbon dioxide concentration in leaves. *Aust. J. Plant Phys., 9*, 121-137, 1982.

Farrell, J. W., and Prell, W. L., Climatic change and $CaCO_3$ preservation: An 800,000-year bathymetric reconstruction from the central equatorial Pacific Ocean. *Paleoceanography, 4*, 447-466, 1989.

Fluegge, A., Molecular-isotopic derivation of maps of sea surface temperatures and paleo-PCO_2 in the eastern equatorial Pacific, M.S. thesis, Ind. Univ., Bloomington, 76 pp., 1994.

Francois, R., M. A. Altabet, R. Goericke, D. C. McCorkle, C. Brunet, and A. Poisson, Changes in the $\delta^{13}C$ of surface water particulate organic matter across the subtropical convergence in the S.W. Indian Ocean, *Global Biogeohem. Cycles, 7*, 627-644, 1993.

Freeman, K. H., and J. M. Hayes, Fractionation of carbon isotopes by phytoplankton and estimates of ancient CO_2 levels, *Global Biogeochem. Cycles, 6*, 185-198, 1992.

Freeman, K. H., J. M. Hayes, J.-M. Trendel, and P. Albrecht, Evidence from carbon isotope measurements for diverse origins of sedimentary biomarkers, *Nature, 353*, 254-256, 1990.

Goericke, R., and B. Fry, Variations in marine plankton $\delta^{13}C$ with latitude, temperature, and dissolved CO_2 in the world ocean, *Global Biogeochem. Cycles, 8*, 85-90, 1994.

Goericke, R., J. P. Montoya, and B. Fry, Physiology of isotope fractionation in algae and cyanobacteria, in *Stable Isotopes in Ecology*, chap. 9, 187-221, edited by K. Lajtha and B. Michener, Academic, San Diego, Calif., 1993.

Hayes, J. M., Factors controlling ^{13}C contents of sedimentary organic compounds: Principles and evidence, *Mar. Geol., 113*, 111-125, 1993.

Hayes, J. M., and J. P. Jasper, Relationships between CO_2 levels and ^{13}C in organic matter, an overview and prospects, paper presented at the 16th Meeting on Organic Geochemistry, Meeting Sponsor, European Association of Organic Geochemists, Stavanger, Norway, 1993.

Hayes, J. M., K. H. Freeman, B. N. Popp, and C. H. Hoham, Compound-specific isotopic analyses, a novel tool for reconstruction of ancient biogeochemical processes, *Org. Geochem., 16*, 1115-1128, 1990.

Hemleben, C., M. Spindler, and O.R. Anderson, *Modern Planktonic Foraminifera*, 363 pp., Springer-Verlag, New York, 1989.

Imbrie J., J. D. Hays, D. G. Martinson, A. McIntyre, A. Mix, J. J. Morley, N. G. Pisias, W. G. Prell, and N. J. Shackleton, The orbital theory of Pleistocene climate: Support from a revised chronology of the marine $\delta^{18}O$ record, in *Milankovitch and Climate, Part 1*, edited by A. L. Berger et al., pp. 269-305, D. Reidel, Hingham, Mass., 1984.

Imbrie J., A. McIntyre, and A. C. Mix, Oceanic response to orbital forcing in the late Quaternary: Observational and experimental strategies, in *Climate and Geosciences*, edited by A. L. Berger et al., pp. 121-164, Kluwer Academic, Boston. Mass., 1989.

Jasper, J. P., and R. B. Gagosian, Alkenone molecular stratigraphy in an oceanic environment affected by glacial meltwater events, *Paleoceanography, 4(6)*, 603-614, 1989.

Jasper, J. P., and J. M. Hayes, A carbon isotope record of CO_2 levels during the late Quaternary, *Nature, 347*, 462-464, 1990.

Jasper, J. P., J. M. Hayes, L.D. Keigwin, and E. L. Sikes, Molecular isotopic evidence of deglacial decline of c_e in the North Atlantic and control of Late Quaternary atmospheric pCO_2, paper presented at Third Meeting of The Oceanography Society, The Oceanography Society, Seattle, Wash., 1993.

Jouzel, J., N.I. Barkov, J. M. Barnola, M. Bender, J. Chapellaz, C. Genthon, V. M. Kotlyakov, V. Lipenkov, C. Lorius, J. R. Petit, D. Raynaud, G. Raisbeck, C. Ritz, T. Sowers, M. Stievenard, F. Yiou, and P. Yiou, Vostok ice cores: Extending the climatic records over the penultimate glacial period, *Nature, 364*, 407-412, 1993.

Keeling, D., R. B. Bacastow, A. F. Carter, S. C. Piper, T. P. Whorf, M. Heimann, W. G. Mook, and H. Roeloffzen, A three-dimensional model of atmospheric CO_2 transport based on obseved winds, I, Analysis of observational data, *Aspects of Climate Variability in the Pacific and Western Americas, Geophys. Monogr. Ser.*, vol. 55, edited by D. H. Peterson, pp. 165-235, AGU, Washington, D. C., 1989.

Keir, R. S., Cold surface ocean ventilation and its effect on atmospheric CO_2, *J. Geophys. Res., 98*, 849-856, 1993.

Levitus, S., Climatological Atlas of the World Ocean, Prof. Pap. 13, Natl. Oceanic and Atmos. Admin., Rockville, Md., 1982.

Lyle, M., D. M. Murray, B. P. Finney, J. Dymond, J. M. Robbins, and K. Brooksforce, The record of late Pleistocene biogenic sedimentation in the eastern tropical Pacific Ocean. *Paleoceanography, 3*, 39-59, 1988.

Lyle, M., F. G. Prahl, and M. A. Sparrow, Upwelling and productivity changes inferred from a temperature record in the central equatorial Pacific, *Nature, 355*, 812-815, 1992.

Martinson, D., N. G. Pisias, J. D. Hays, J. Imbrie, T. C. Moore Jr., and N. J. Shackleton, Age dating and orbital theory of the ice ages: Development of a high-resolution 0 to 300,000 year chronostratigraphy, *Quat. Res., 27*, 1-27, 1987.

McCabe, B., The dynamics of ^{13}C in several New Zealand Lakes, Ph.D. thesis, 278 pp., Univ. of Waikato, 1985.

Mix, A. C., N. G. Pisias, R. Zahn, W. Rugh, C. Lopez, and K. Nelson, Carbon 13 in Pacific deep and intermediate waters, 0-370 ka: Implications for ocean circulation and Pleistocene CO_2, *Paleoceanography, 6*, 205-226, 1991.

Mook, W. G., J. C. Bommerson, and W. H. Staberman, Carbon isotope fractionation between dissolved bicarbonate and gaseous carbon dioxide, *Earth Planet. Sci. Letters, 22*, 169-176, 1974.

Morse, J. W., and F. T. Mackenzie, Geochemistry of sedimentary carbonates, *Dev. Sedimentol.*, vol. 48, 417 pp., Elsevier, New York, 1990.

Murphy, P. P., R. A. Feeley, R. H. Gammon, D. E. Harrison, K. C. Kelly, and L. S. Waterman, Assessment of the air-sea exchange of CO_2 in the South Pacific during austral autumn, *J. Geophys. Res., 96*, 20,455-20,465, 1991.

Murray, D. W., Spatial and temporal variations in sediment accumulation in the central equatorial Pacific, Ph.D. thesis, 198 pp., Oregon State Univ., Corvallis, 1987.

Murray, J. W., R. A. Feeley, and M. S. Leinen, Cruises are over, results are coming in for U.S. EqPac study, *U.S. JGOFS News, 4*, 1-2, 6-7, 1993.

Neftel, A., E. Moor, H. Oeschger, and B. Stauffer, Evidence from polar ice cores for the increase in atmospheric CO_2 in the past two centuries, *Nature, 315*, 45-47, 1985.

Opdyke, B. N., and J. C. G. Walker, Return of the coral reef hypothesis: Basin to shelf partitioning of $CaCO_3$ amd its effect on atmospheric CO_2, *Geology, 20*, 733-736, 1992.

Pedersen, T. F., Increased productivity in the eastern equatorial Pacific during the last glacial maximum (19,000 to 14,000 yr B.P.), *Geology, 11*, 16-19, 1983.

Pedersen, T. F., M. Pickering, J. S. Vogel, J. N. Southon, and D. E. Nelson, The response of benthic foraminifera to productivity cycles in the eastern Equatorial Pacific: Faunal and geochemical constraints on glacial bottom water oxygen levels, *Paleoceanography, 3*, 157-168, 1988.

Pedersen, T. F., B. Nielsen, and M. Pickering, Timing of late Quaternary productivity pulses in the Panama Basin and implications for atmospheric CO_2. *Paleoceanography, 6*, 657-677, 1991.

Petit, J. R., L. Mounier, J. Jouzel, Y. S. Korotkevich, V.I. Kotlyakov, and C. Lorius, Palaeoclimatological and chronological implications of the Vostok core dust record, *Nature, 343*, 56-58, 1990.

Popp, B. N., R. Takigiku, J. M. Hayes, J. W. Louda, and E. W. Baker, The post-Paleozoic chronology and mechanism of ^{13}C depletion in primary marine organic matter, *Am. J. Sci., 289*, 436-454, 1989.

Prahl, F. G., L. A. Muehlhausen, and D. L. Zahnle, Further evaluation of long-chain alkenones as indicators of paleoceanographic conditions, *Geochim. Cosmochim. Acta, 52*, 2303-2310, 1988.

Prahl, F. G., L. A. Muehlhausen, and M. Lyle, An organic geochemical assessment of oceanographic conditions at MANOP Site C over the past 26,000 years, *Paleoceanography, 4*, 495- 510, 1989.

Prahl, F.G. and Wakeham, S.G., Calibration of unsaturation patterns in long-chain ketone compositions for palaeotemperature assessment. *Nature, 330*, 367-369, 1987.

Quay, P. D., B. Tilbrook, and C. S. Wong, Oceanic uptake of fossil fuel CO_2: Carbon-13 evidence, *Science, 256*, 74-79, 1992.

Rau, G. H., P. N. Froelich, T. Takahashi, and D. J. DesMarais, Does sedimentary organic $\delta^{13}C$ record variation in Quaternary ocean c_e?, *Paleoceanography, 6*, 335-347, 1991.

Rau, G. H., T. Takahashi, D. J. DesMarais, D. J. Repeta, and J. H. Martin, The relationship between the $\delta^{13}C$ of organic matter and c_e in ocean surface water: Data from a JGOFS site in the northeast Atlantic Ocean and a model, *Geochim. Cosmochim. Acta, 56*, 1413-1419, 1992.

Ravelo, C., R. G. Fairbanks, and S. G. H. Philander, Reconstructing tropical Atlantic hydrography using planktonic foraminifera and an ocean model, *Paleoceanography, 5*, 409-431, 1990.

Raven, J. A., and A. M. Johnston, Mechanisms of an organic-carbon acquisition in marine phytoplankton and their implications for the use of other resources, *Limnol. Oceanogr., 36*, 1701-1714, 1991.

Sarnthein, M., K. Winn, J.-C. Duplessy, and M. R. Fontugne, Global variations of surface ocean productivity in low and mid latitudes: Influence on CO_2 reservoirs of the deep ocean and atmosphere during the last 21,000 years, *Paleoceanography, 3*, 361-399, 1988.

Shackleton, N. J. and N. G. Pisias, Atmospheric carbon dioxide, orbital forcing, and climate, in *The Carbon Cycle and Atmospheric CO_2: Natural Variations Archean to Present, Geophys. Monogr. Ser.*, vol. 32, edited by E. T. Sundquist and W. S. Broecker, pp. 303-318, AGU, Washington, D. C., 1985.

Shackleton, N. J., J. Le, A. Mix, and M. A. Hall, Carbon isotope records from Pacific surface waters and atmospheric carbon dioxide, *Quat. Sci. Rev., 11*, 387-400, 1992.

Shackleton, N. J., M. A. Hall, J. Line, and C. Shuxi, Carbon isotope data in core V19-30 confirm reduced carbon dioxide concentration in the ice age atmosphere, *Nature, 306*, 319-322, 1983.

Skirrow, G., The dissolved gases—Carbon dioxide, in *Chemical Oceanography*, vol. 2, 2nd ed., edited by J. P. Riley and G. Skirrow, pp. 1-192, Academic, San Diego, Calif., 1975.

Spero, H., I. Lerche, and D.F. Williams, Opening the carbon isotope "vital effect" black box, 2, Quantitative model for interpreting foraminiferal carbon isotope data, *Paleoceanography, 6*, 639-655, 1991.

Stauffer, B., H. Hofer, H. Oeschger, J. Schwander, and U. Siegenthaler, Atmospheric CO_2 concentration during the last glaciation, *Ann. Glaciol., 5*, 160-164, 1984.

Tans, P. P., I. Y. Fung, and T. Takahashi, Observational constraints on the global atmospheric CO_2 budget, *Science, 247*, 1431-1438, 1990.

Volk, T. and R. Bacastow, The changing patterns of ΔpCO_2 between ocean and atmosphere, *Global Biogeochem. Cycles, 3,* 179-189, 1989.

Wakeham, S. G., D. J. Hollander, and J. M. Hayes, Biogeochemical dynamics of ^{13}C in marine POC and related sterols, paper presented at Third Meeting of The Oceanography Society,The Oceanography Society, Seattle, Wash., 1993.

Weiss, R. F. Carbon dioxide in water and seawater: The solubility of a non ideal gas, *Mar. Chem.,* 2, 203-215, 1974.

J.M. Hayes, Biogeochemical Laboratories, Indiana University, Bloomington, IN 47405-1403. (e-mail: biogeo@indiana.edu)

J.P. Jasper, Department of Marine Sciences, University of Connecticut, Groton, CT 06340.

A.C. Mix and F.G. Prahl, College of Oceanography, Oregon State University, Corvallis, OR 97331. (e-mail: mix@oce.orst.edu and prahl@oce.orst.edu)

(Received January 21, 1993; revised August 11, 1994; accepted August 11, 1994.)